Catalytic C(sp^2)–H Amination Reactions Using Dinickel Imides

Supporting Information

Ian G. Powers, John M. Andjaba, Matthias Zeller, and Christopher Uyeda*

Department of Chemistry, Purdue University, 560 Oval Dr., West Lafayette, IN 47907, USA

1. Spectroscopic and Cyclic Voltammetric Data for Dinickel Complexes

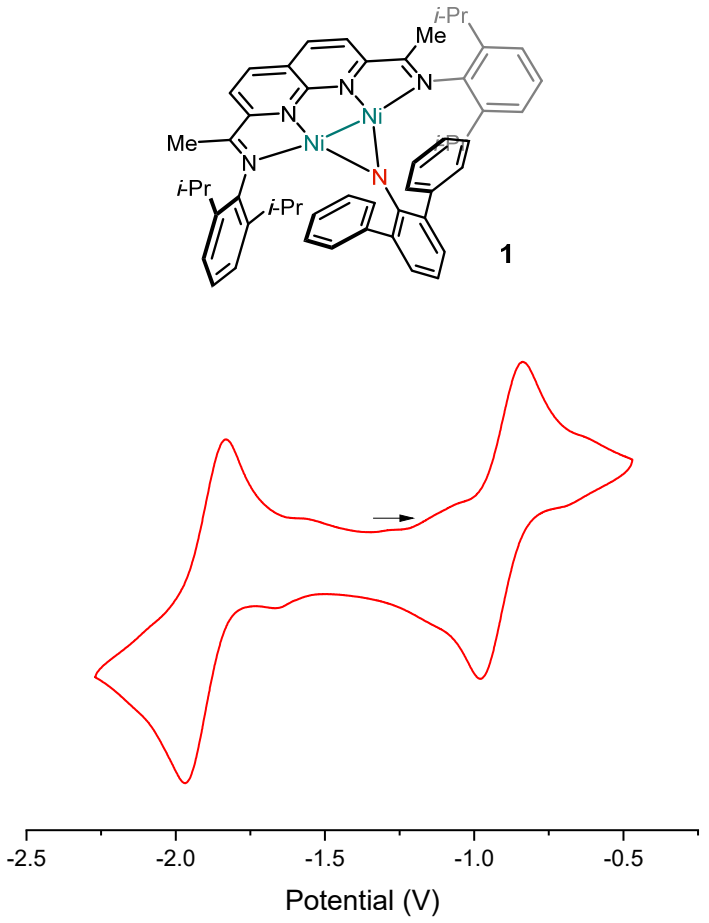

Figure S1. Cyclic voltammogram for ($^{i\text{-Pr}}$NDI)Ni$_2$(μ-NAr) (**1**) (0.3 M [*n*-Bu$_4$N][PF$_6$] supporting electrolyte in THF, glassy carbon working electrode, 100 mV/s scan rate). The scan begins at the open circuit potential and proceeds in the indicated direction.

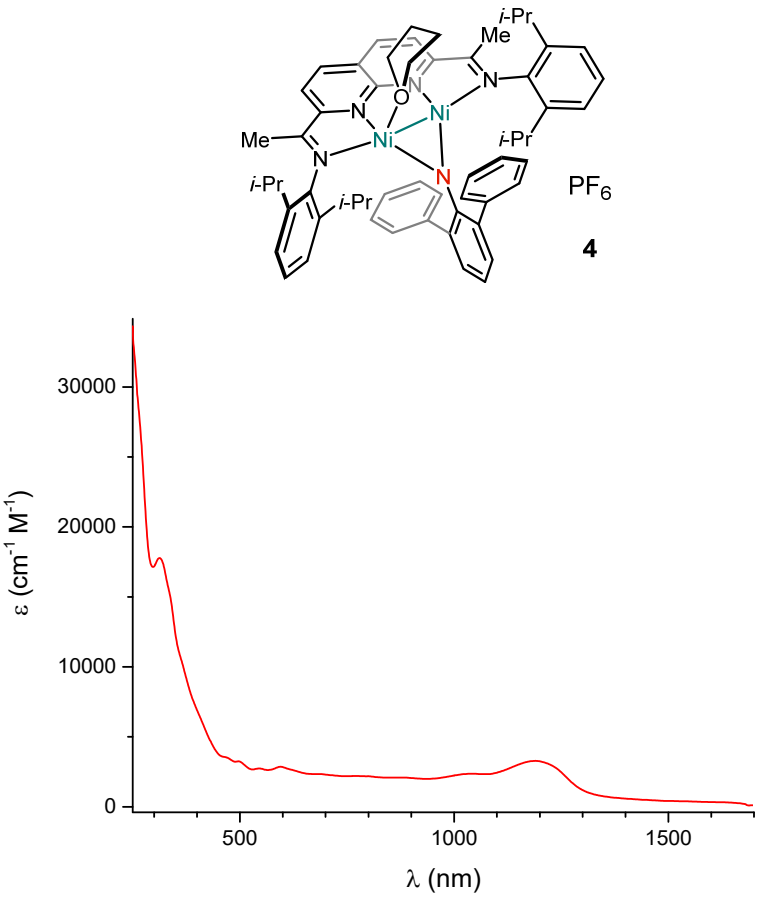

Figure S2. UV–vis–NIR spectrum of **4** in THF (0.128 mM).

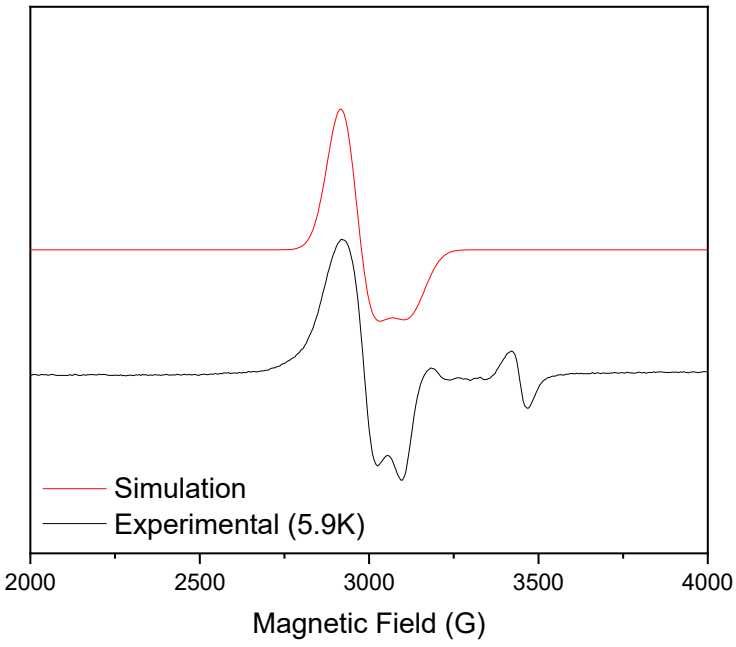

Figure S3. Frozen solution (5.9 K, THF) X-band EPR spectrum for **4**. Simulated parameters: g_1 = 2.341, g_2 = 2.206. $g_{max} - g_{min}$ = 0.135. The signal at g = 2.0 is attributed to an uncharacterized *S* = 1/2 impurity.

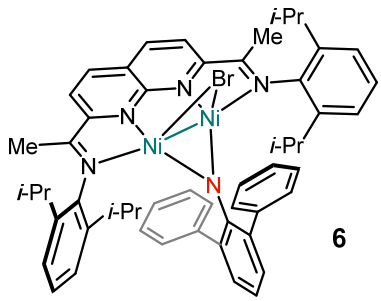

6

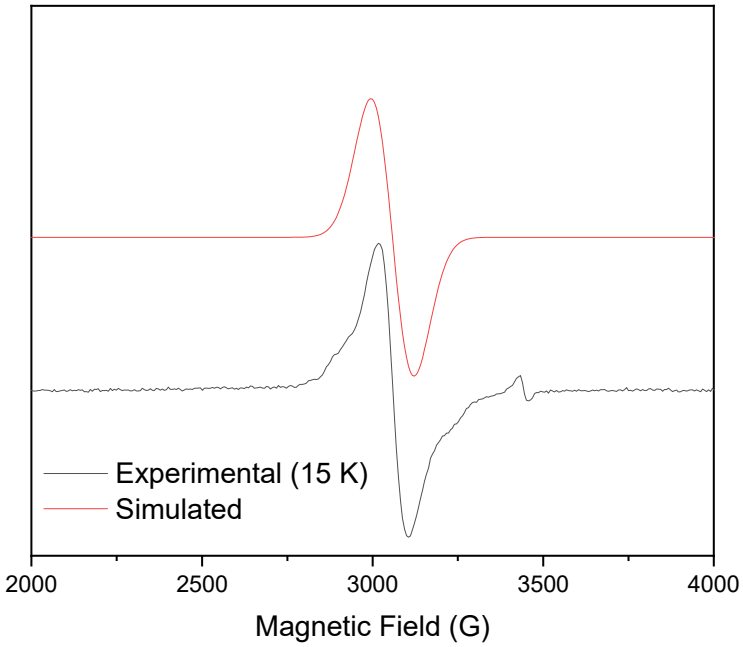

Figure S4. Frozen solution (15 K, THF) X-band EPR spectrum for **6**. Simulated parameters: g_1 = 2.254.

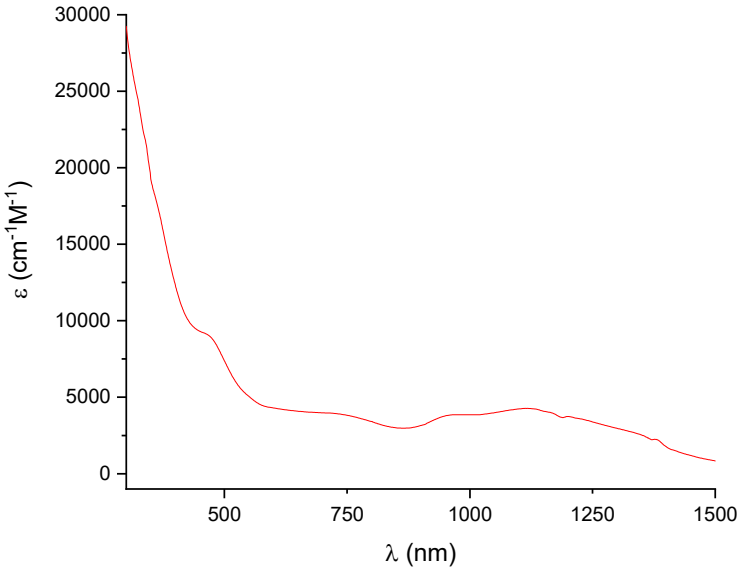

Figure S5. UV-vis-NIR spectrum of **6** in THF (0.057 mM).

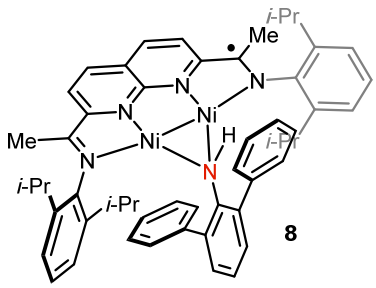

8

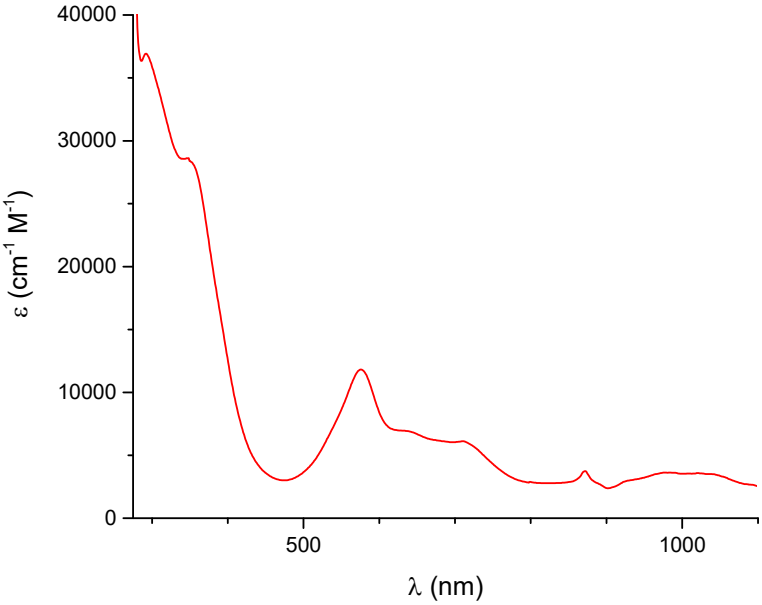

Figure S6. UV-Vis-NIR spectrum of **8** in C_6H_6 (0.067 mM).

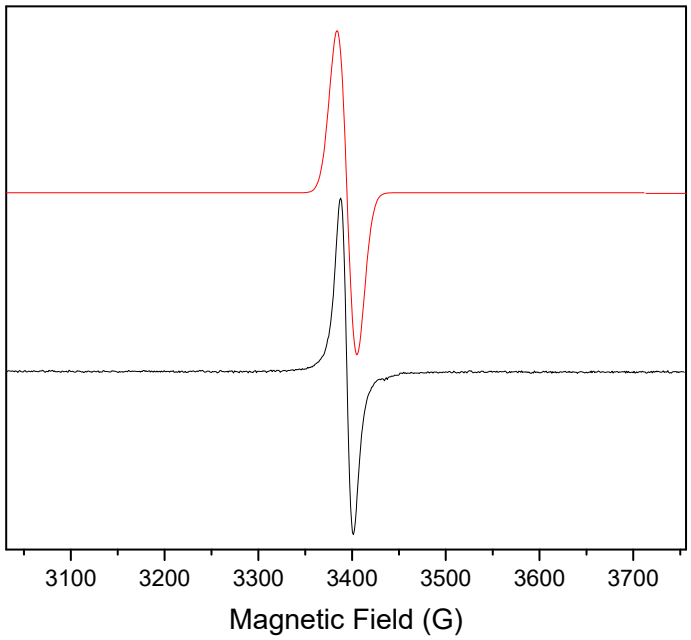

Figure S7. Solution (298 K, toluene) X-band EPR spectrum for **8**. Simulated parameters: g_{iso} = 2.071.

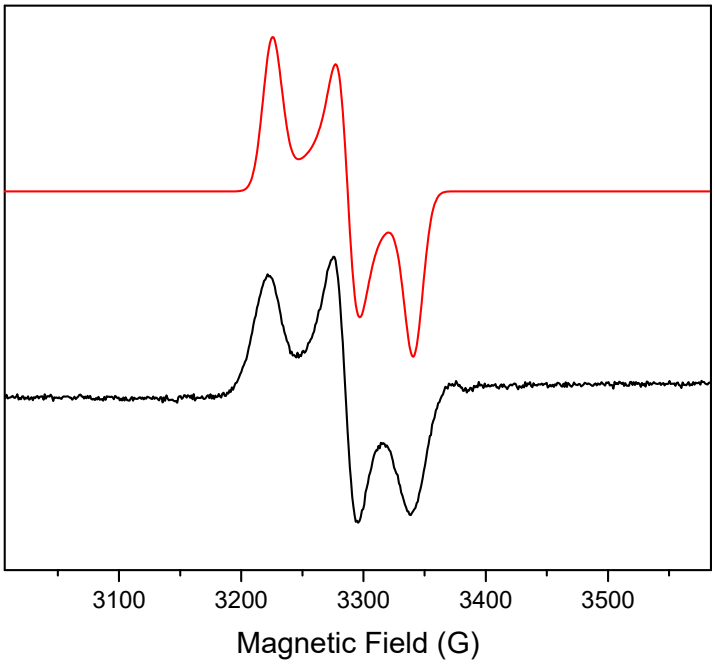

Figure S8. Frozen solution (108 K, toluene) X-band EPR spectrum for **8**. Simulated parameters: g_1 = 2.032 g_2 = 2.066 g_3 = 2.105. $g_{max} - g_{min}$ = 0.073.

2. Stoichiometric Decomposition Reactions of Dinickel Complexes

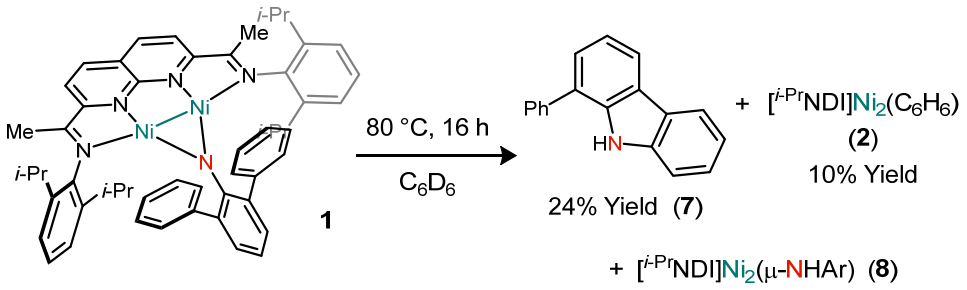

Stoichiometric decomposition of Compound 1. In an N_2 filled glovebox, a J-Young NMR tube was charged with **1** (12.5 mg, 0.014 mmol, 1.0 equiv), *m*-terphenylazide (3.7 mg, 0.014 mmol, 1.0 equiv), and C_6D_6, along with 1,3,5-trimethoxybenzene (2.1 mg, 0.013 mmol) as an internal standard. After mixing for 10 min, the brown reaction mixture was heated at 80 °C for 16 h resulting in a color change to dark blue. The yields of 1-phenyl-9-H-carbazole (**7**) and recovered **2** were determined by ^{1}H NMR integration against the internal standard (24% and 10%, respectively). Complex **8** was identified as the major $S = 1/2$ compound by EPR and UV-Vis.

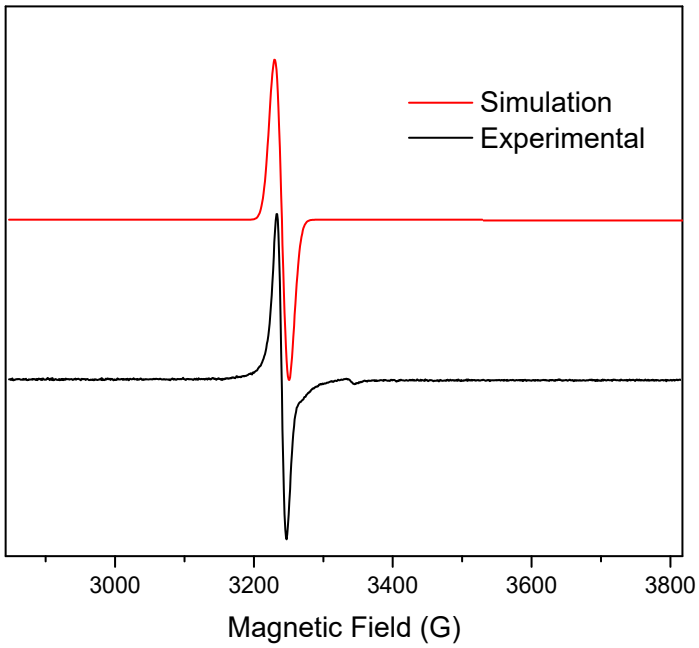

Figure S9. EPR spectrum for the decomposition of **1** (298 K, C_6H_6). Simulated parameters g_{iso} = 2.068.

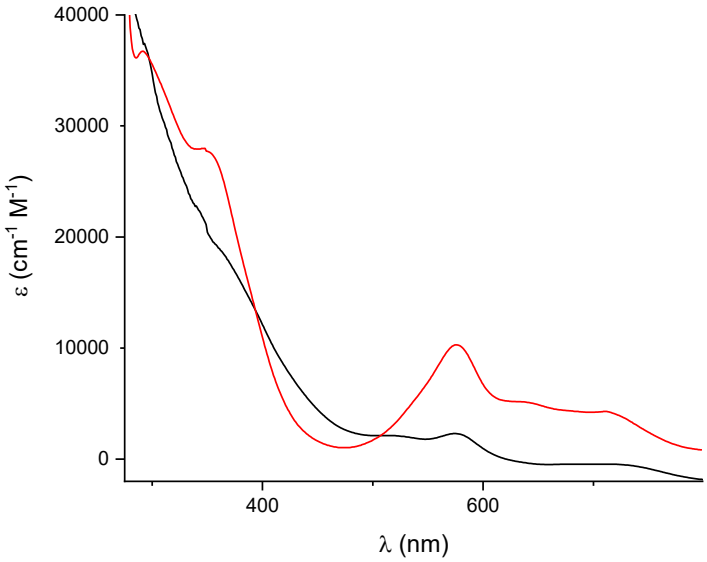

Figure S10. UV-Vis spectrum for the decomposition of **1** in C_6H_6 (0.073 mM) in black overlaid with spectrum of isolated **8** in C_6H_6 (0.067 mM) in red.

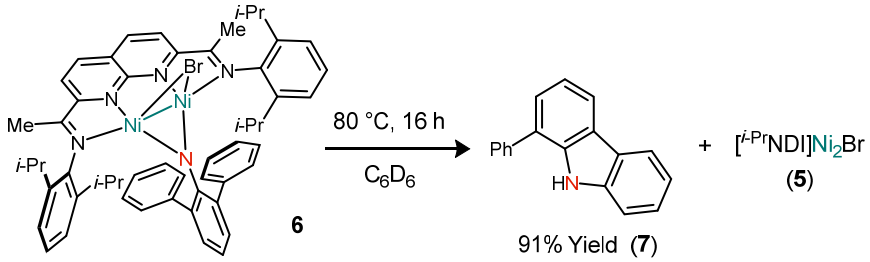

Stoichiometric decomposition of Compound 6. In an N_2 filled glovebox, a J-Young NMR tube was charged with **6** (9.4 mg, 0.0097 mmol) and C_6D_6 (1.0 mL) along with 1,3,5-trimethoxybenzene (2.2 mg, 0.013 mmol) as an internal standard. After mixing for 10 min, the reaction mixture was heated at 80 °C for 16 h. The yield of 1-phenyl-9-H-carbazole (**7**) was determined to be 91% by ^{1}H NMR integration against the internal standard. Complex **5** was identified as the primary $S = 1/2$ product by EPR.

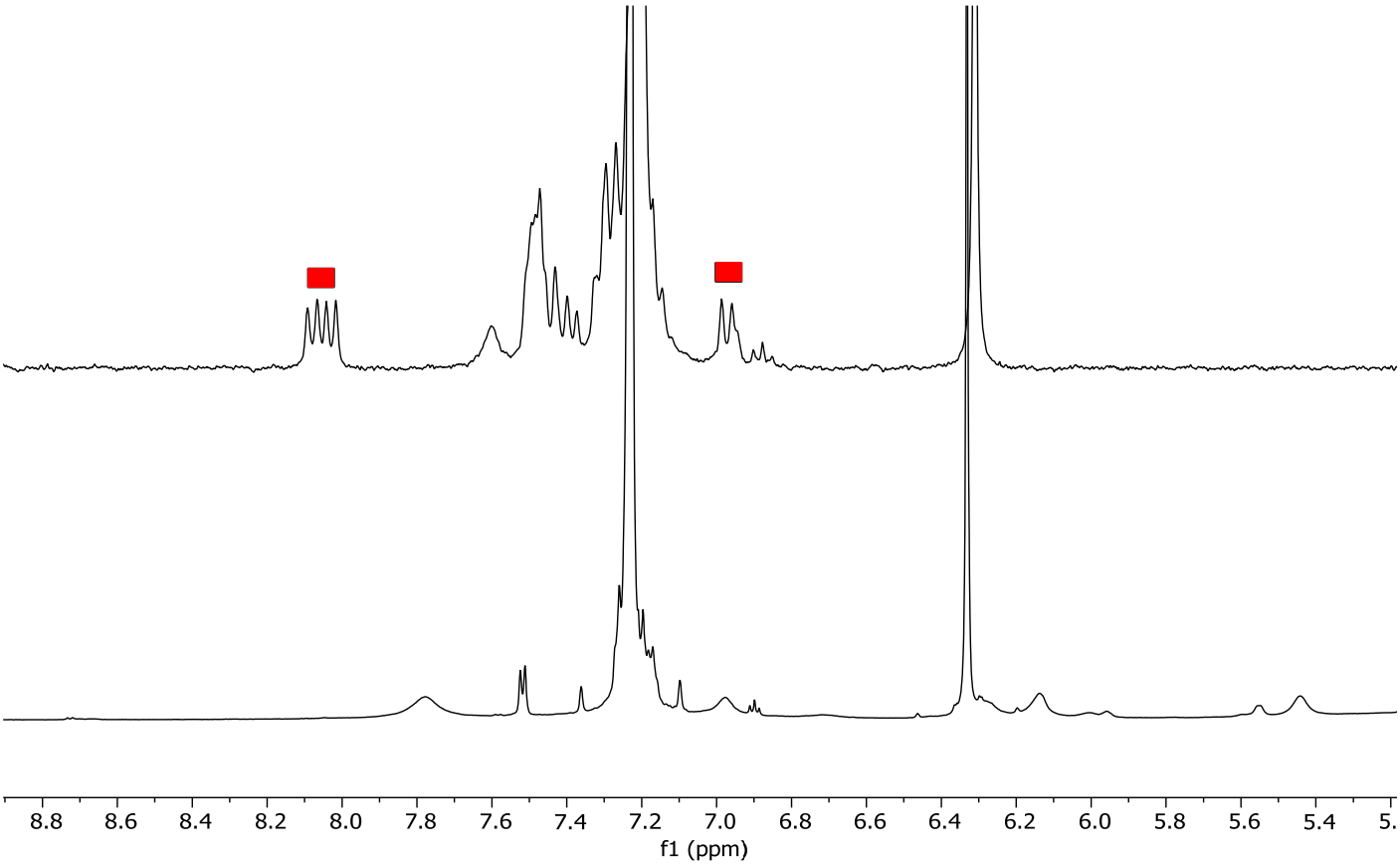

Figure S11. Initial ^{1}H NMR spectrum of **6** (bottom) and of **6** after heating at 80 °C for 16 h (top). Red squares indicate peaks corresponding to **7.**

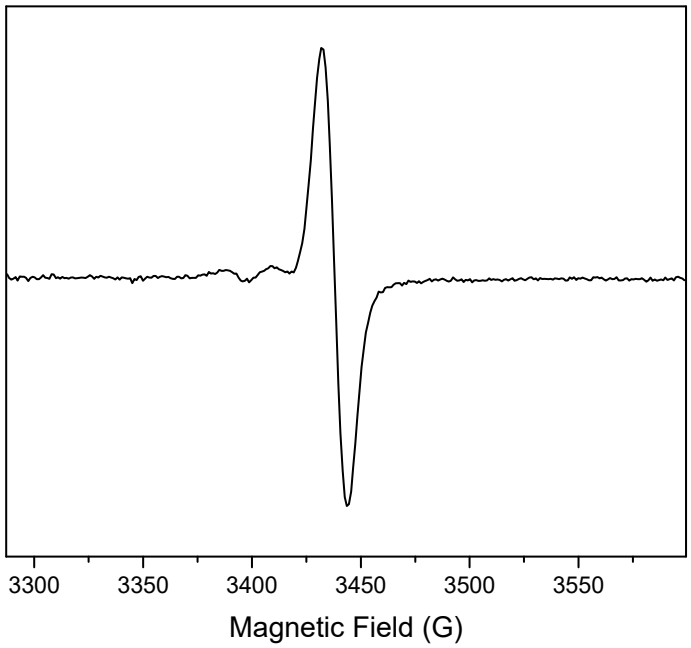

Figure S12. EPR spectrum after heating **6** at 80 °C for 16 h. Simulated parameters g_{iso} = 2.04.

3. Catalytic C–H Amination Reactions of 3

General Procedure. In an N_2 filled glovebox, a J-Young NMR tube was charged with catalyst (10 mol%), *m*-terphenylazide (3.0 mg, 0.011 mmol) 1,3,5-trimethoxybenzene (1.9 mg, 0.011 mmol) as an internal standard, and toluene-d_8 (700 µL). The reaction was heated at 80 °C for 72 h. The yields of indole **7** and aniline **10** were determined by ^{1}H NMR integration against the internal standard.

Procedure for entry 5. In an N_2 filled glovebox, a J-Young NMR tube was charged with **2** (0.95 mg, 0.0013mmol, 5 mol%), $[Cp_2Fe]PF_6$ (0.43 mg, 1.0 equiv), *m*-terphenylazide (3.0 mg, 0.011 mmol), 1,3,5-trimethoxybenzene (1.9 mg, 0.011 mmol) as an internal standard, and toluene-d_8 (700 µL). The reaction was heated at 110 °C for 24 hours. The yields of indole **7** and aniline **10** were determined by ^{1}H NMR integration against the internal standard.

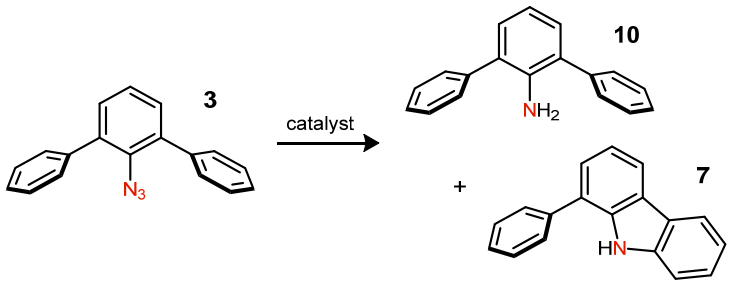

entry	catalyst	Yield of **7**	Yield of **10**
1	Ni_2(µ-NAr) **1**	39%	33%
2	Ni_2(µ-NHAr) **8**	44%	39%
3	Ni_2(µ-Br) **5**	77%	16%
4	$[Ni_2(\mu\text{-NAr})(thf)]^+$ **4**	89%	6%
5[a]	$[Ni_2(\mu\text{-NAr})(thf)]^+$ **4**	87%	6%
6[b]	$[Ni_2(\mu\text{-NAr})(thf)]^+$ **4**	96%	<2%

Figure S13. [a]See procedure above. [b]Reaction conditions: 5 mol% catalyst at 110 °C for 24 h.

4. Synthesis of Azide Compounds and C–H amination Reactions

Safety Note. Though no specific safety concerns arose during our studies, organoazide compounds are high energy molecules, and they are known to be thermally unstable and shock sensitive. In order to minimize explosion hazards, general care should be taken to avoid organoazides with low C-to-N ratios, limit scale to the extent possible, and store organoazides in solution.

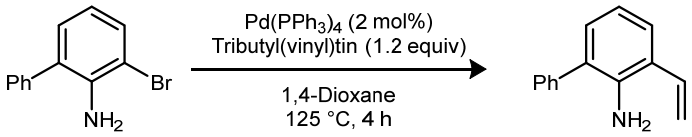

3-vinyl-[1,1'-biphenyl]-2-amine. The following procedure was adapted from a previously reported method.[1] In an N_2 filled glovebox, a Schlenk flask was charged with 3-bromo-[1,1'-biphenyl]-2-amine (298 mg, 1.2 mmol), $Pd(PPh_3)_4$ (2.8 mg, 0.024 mmol, 2 mol %), tributyl(vinyl)tin (0.42 mL, 1.45 mmol), and anhydrous 1,4-dioxane (9 mL). The reaction vessel was sealed, removed from the glovebox, and heated at 125 °C. After 4 h, the reaction mixture was cooled to room temperature, and 10% KF (aq) solution (0.08 M, 22.5 mL) was added. The mixture was allowed to stand for 2 h then filtered through a pad of celite. The filtrate was extracted with 2 × 10 mL of ether, and the combined organic phases were washed with sat. NaCl (aq) (10 mL), dried over Na_2SO_4, and concentrated under reduced pressure. The crude product was directly loaded onto a SiO_2 column for purification (2.5:97.5 EtOAc: hexane). The product was isolated as a yellow oil (0.212 g, 92% yield).

^{1}H NMR (300 MHz, $CDCl_3$) δ 7.27 (s, 2H), 7.23 – 7.04 (m, 4H), 6.89 (dd, *J* = 7.4, 1.6 Hz, 1H), 6.72 – 6.57 (m, 2H), 5.49 (dt, *J* = 17.4, 1.5 Hz, 1H), 5.18 (dd, *J* = 10.9, 1.5 Hz, 1H), 3.67 (s, 2H).

^{13}C{^{1}H} NMR (201 MHz, $CDCl_3$) δ 141.0, 139.6, 133.3, 130.1, 129.4, 129.0, 128.6, 128.4, 127.4, 126.9, 124.7, 122.0, 120.2, 118.6, 116.5, 29.9

HRMS(ESI): calcd for $C_{14}H_{13}N^+$: 196.1121; found: 196.1123

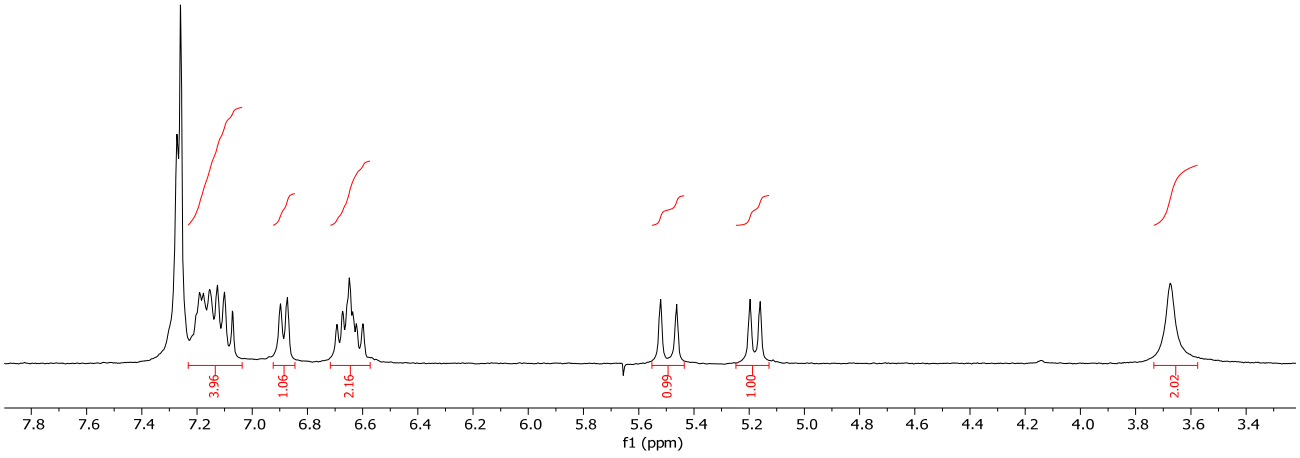

Figure S14. ^{1}H NMR spectrum for 3-vinyl-[1,1'-biphenyl]-2-amine in $CDCl_3$.

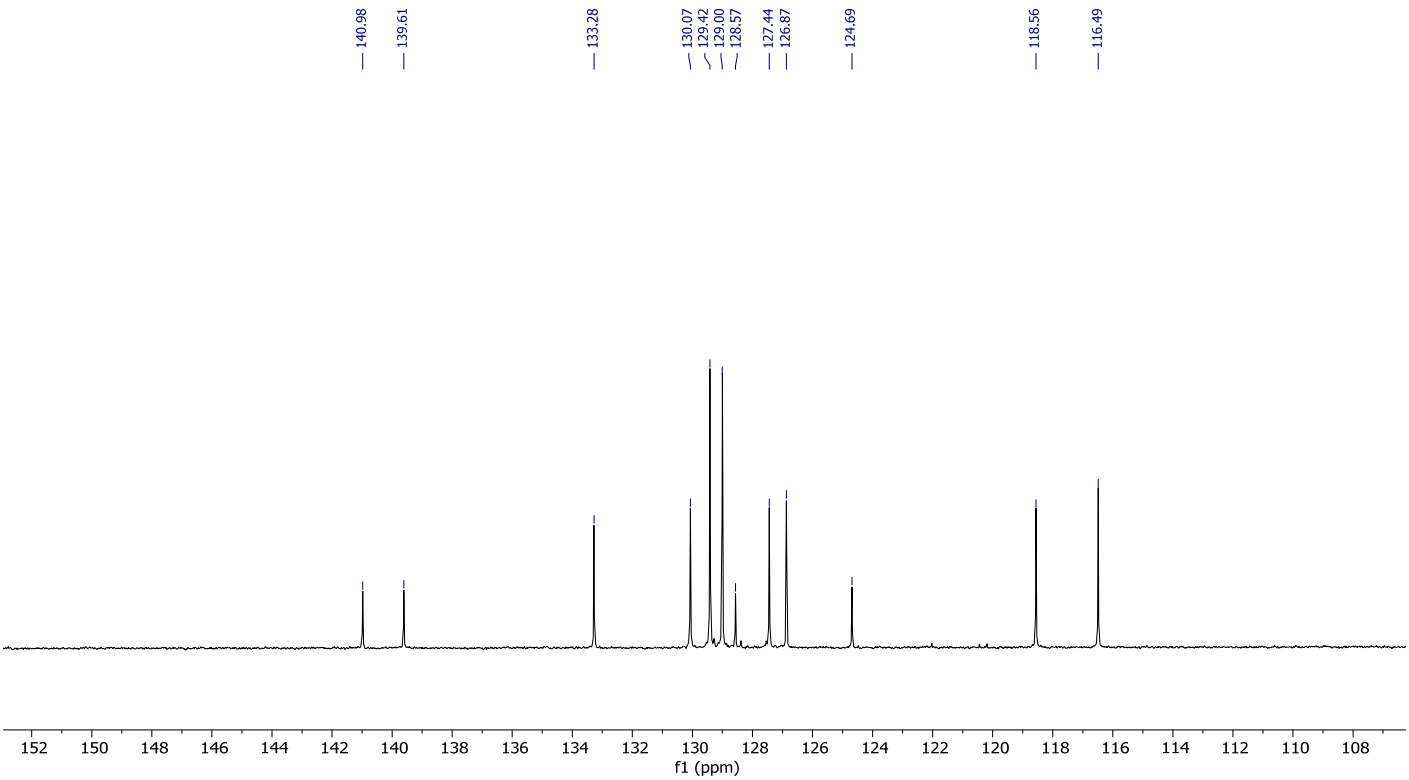

Figure S15. $^{13}C\{^{1}H\}$ NMR spectrum for 3-vinyl-[1,1'-biphenyl]-2-amine in $CDCl_3$.

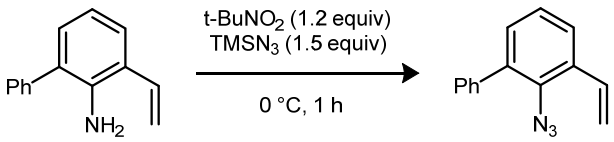

2-azido-3-vinyl-1,1'-biphenyl (17). A solution of 3-vinyl-[1,1'-biphenyl]-2-amine (330 mg, 1.69 mmol, 1.0 equiv) in CH_3CN (8.5 mL) was cooled to 0 °C. *t*-$BuNO_2$ (0.303 mL, 1.2 equiv) and $TMSN_3$ (0.27mL, 1.5 equiv) were added sequentially. The reaction mixture was vigorously stirred at room temperature under air for 1 h. The mixture was concentrated to dryness under reduced pressure. The crude product was directly loaded onto a SiO_2 column for purification (100% hexanes). The product was isolated as a yellow oil (97 mg, 26% yield).

^{1}H NMR (800 MHz, $CDCl_3$) δ 7.52 (dd, *J* = 6.4, 2.9 Hz, 1H), 7.47 (d, *J* = 5.5 Hz, 3H), 7.40 (tt, *J* = 5.7, 3.1 Hz, 1H), 7.24 – 7.19 (m, 2H), 7.11 (dd, *J* = 17.6, 10.9 Hz, 1H), 5.77 (d, *J* = 17.5 Hz, 1H), 5.40 (d, *J* = 11.0 Hz, 1H).

$^{13}C\{^{1}H\}$ NMR (201 MHz, $CDCl_3$) δ 138.1, 136.8, 134.6, 132.4, 132.2, 130.8, 129.2, 128.6, 127.9, 125.8, 125.7, 116.5.

HRMS(ESI): calcd for $C_{14}H_{12}N^{+}$: 194.0964; found: 194.0965.

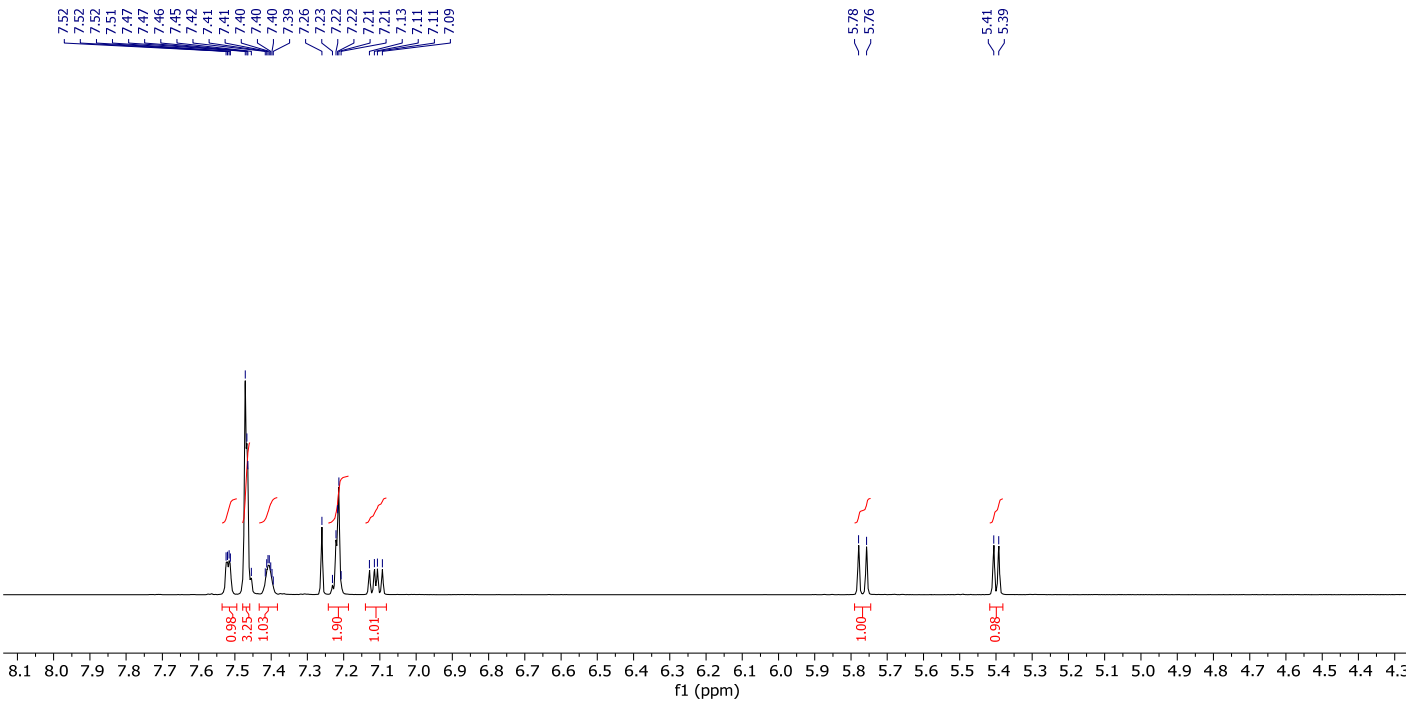

Figure S16. ^{1}H NMR spectrum for **17** in $CDCl_3$.

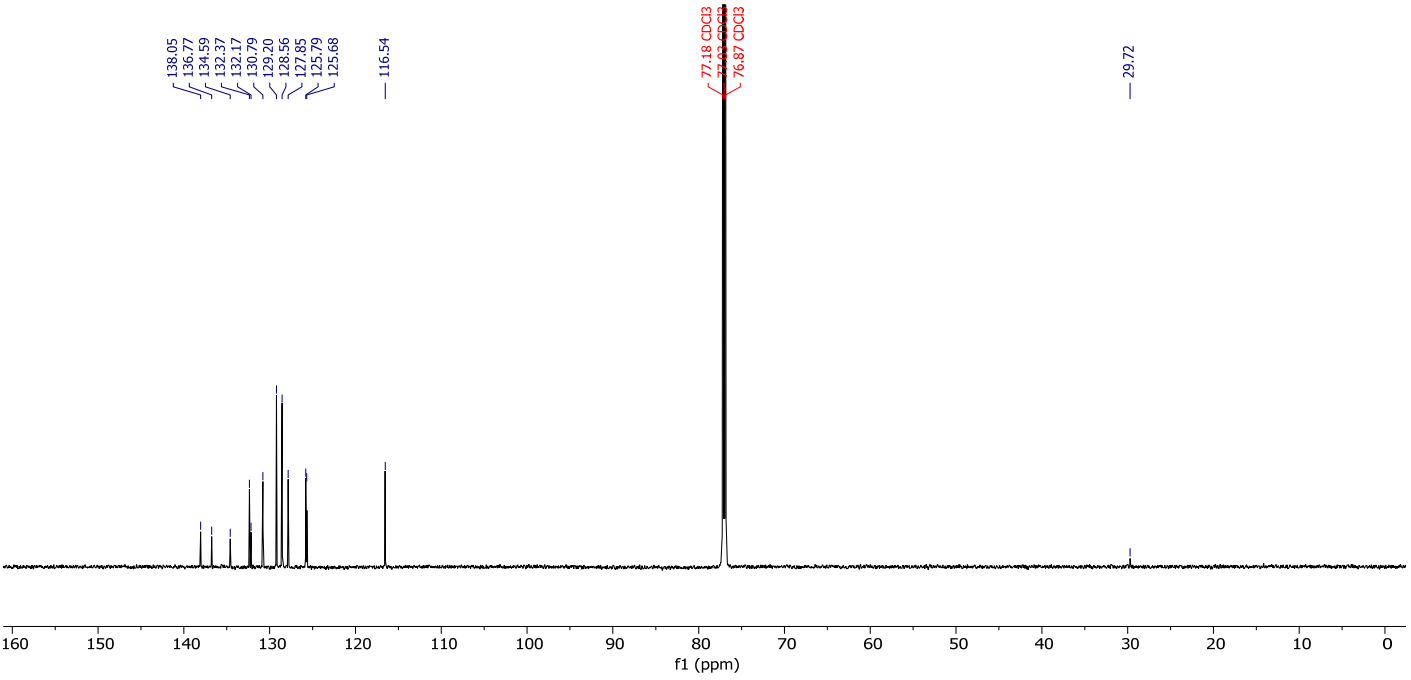

Figure S17. $^{13}C\{^{1}H\}$ NMR spectrum for **17** in $CDCl_3$.

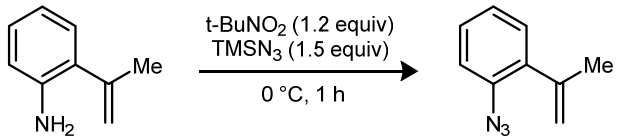

1-Azido-2-(prop-1-en-2-yl)benzene. A solution of 2-(prop-1-en-2-yl)aniline (2.0 g, 15.0 mmol, 1.0 equiv) in CH_3CN (75 mL) was cooled to 0 °C. *t*-$BuNO_2$ (2.69 mL, 1.2 equiv) and $TMSN_3$ (2.39 mL, 1.5 equiv) were added sequentially. The reaction mixture was vigorously stirred at room temperature under air for 1 h. The mixture was concentrated to dryness under reduced pressure. The crude product was directly loaded onto a SiO_2 column for purification (100% hexanes). The product was isolated as a yellow oil (2.39 g, >99% yield).

^{1}H NMR (800 MHz, $CDCl_3$) δ 7.33 (t, *J* = 7.7 Hz, 1H), 7.23 (d, *J* = 7.7 Hz, 1H), 7.18 (d, 1H), 7.13 (t, *J* = 7.7 Hz, 1H), 5.23 (s, 1H), 5.03 (s, 1H), 2.14 (s, 3H).

^{13}C{^{1}H} NMR (201 MHz, $CDCl_3$) δ 143.4, 136.7, 135.8, 129.8, 128.4, 124.8, 118.5, 116.2, 23.6.

HRMS(ESI): calcd for $C_9H_{10}N^+$: 132.0813; found: 132.0805

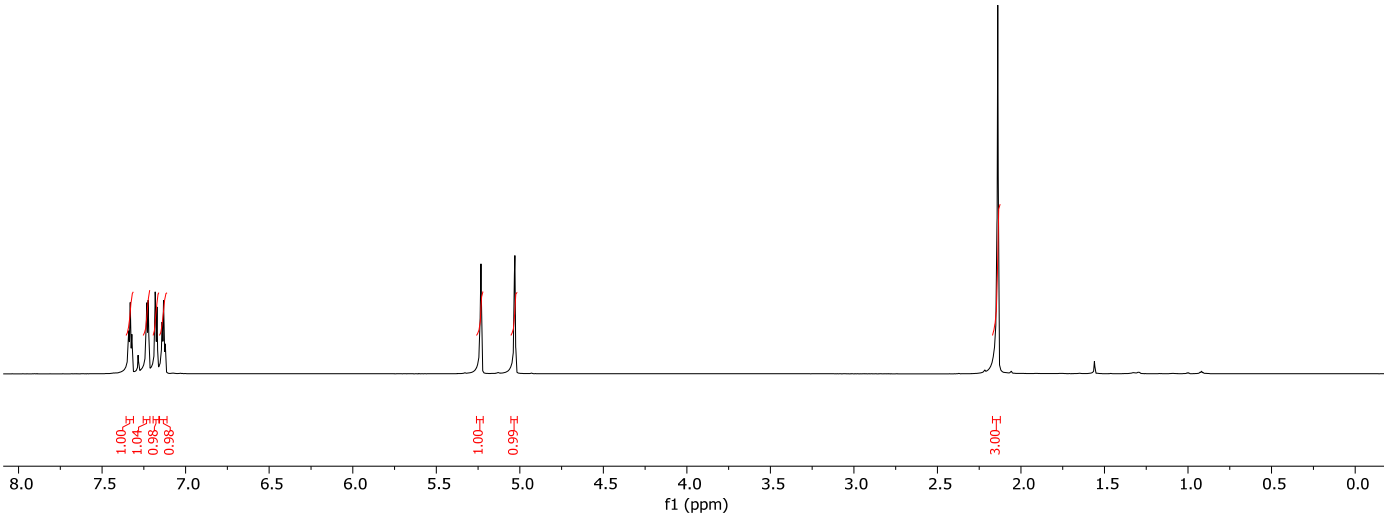

Figure S18. ^{1}H NMR spectrum for 1-azido-2-(prop-1-en-2-yl)benzene in $CDCl_3$.

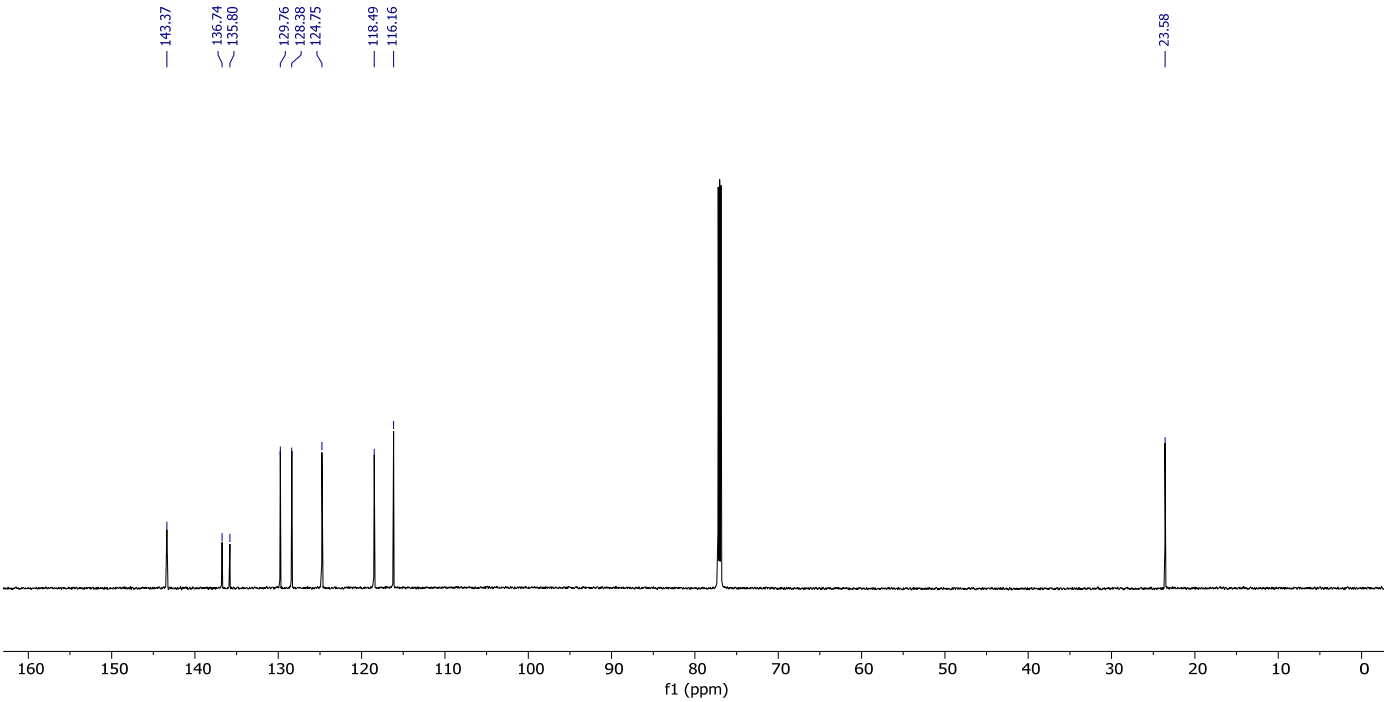

Figure S19. $^{13}C\{^{1}H\}$ NMR spectrum for 1-azido-2-(prop-1-en-2-yl)benzene in $CDCl_3$.

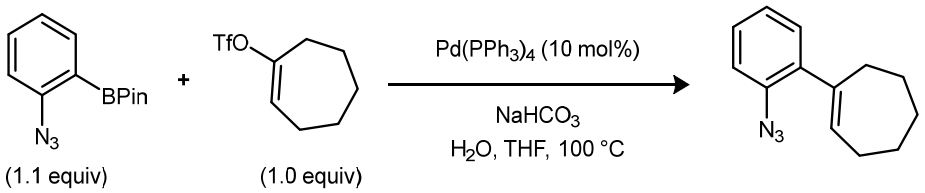

(1-(2-azidophenyl)cyclohept-1-ene). The following procedure was adapted from a previously reported method.[2] In an N_2 filled glovebox, a Schlenk flask was charged with cyclohept-1-en-1-yl trifluoromethanesulfonate (428 mg, 1.8 mmol, 1.0 equiv), 2-azidoarylboronic acid pinacol ester (495 mg, 2.0 mmol, 1.1 equiv), $Pd(PPh_3)_4$ (25 mg, 0.022 mmol, 10 mol %), and 25 mL THF. The flask was sealed, removed from the glovebox, and 6.0 mL of sat. $NaHCO_3$ (aq) was added by syringe. The reaction mixture was heated at 75 °C. After 1 h, the mixture was cooled to room temperature and diluted with 5 mL of water. The solution was extracted with 2 × 10 mL of Et_2O. The combined organic phases were washed with 10 mL of sat. NaCl (aq), dried over Na_2SO_4, and concentrated under reduced pressure. The crude product was directly loaded onto a SiO_2 column for purification (3:97 to 5:95 EtOAc: hexane). The product was isolated as a yellow oil. (300 mg, 80% yield).

^{1}H NMR (800 MHz, $CDCl_3$) δ 7.24 (t, J = 7.6, 1.6 Hz, 1H), 7.13 (d, J = 7.5, 1.6 Hz, 1H), 7.10 (d, J = 8.0, 1.1 Hz, 1H), 7.06 (t, J = 7.5, 1.2 Hz, 1H), 5.84 (t, J = 6.5 Hz, 1H), 2.48 – 2.43 (m, 2H), 2.29 – 2.24 (m, 2H), 1.84 – 1.79 (m, 2H), 1.69 – 1.64 (m, 2H), 1.61 – 1.55 (m, 2H).

$^{13}C\{^{1}H\}$ NMR (201 MHz, $CDCl_3$) δ 143.7, 138.5, 136.7, 132.8, 130.0, 127.7, 124.7, 118.4, 34.5, 32.7, 29.1, 27.0, 26.9.

HRMS(ESI): calcd for $C_{13}H_{16}N^+$: 186.1283; found: 186.1277

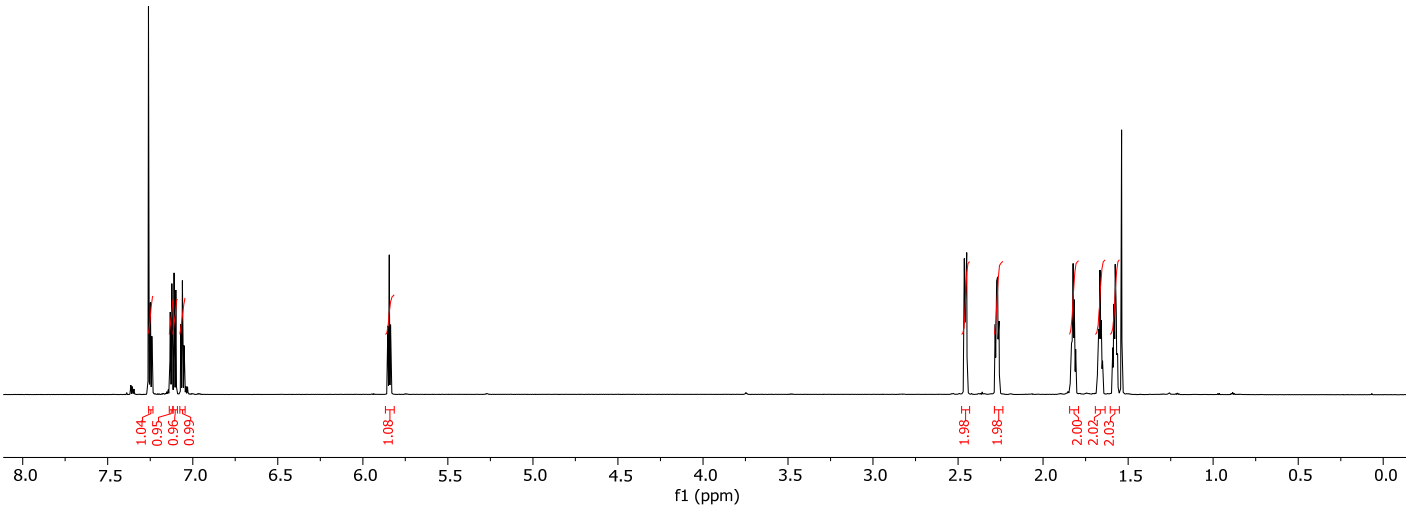

Figure S20. ^{1}H NMR spectrum for (1-(2-azidophenyl)cyclohept-1-ene) in $CDCl_3$.

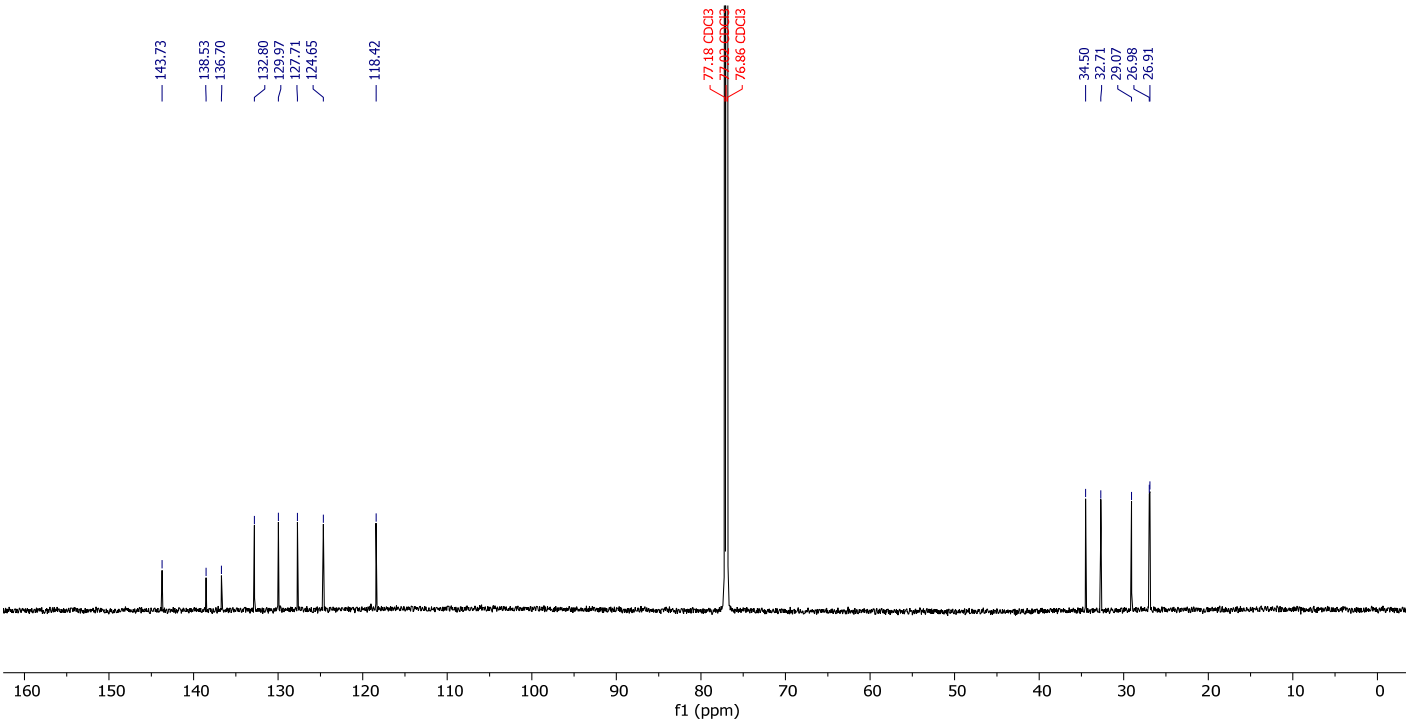

Figure S21. $^{13}C\{^{1}H\}$ NMR spectrum for (1-(2-azidophenyl)cyclohept-1-ene) in $CDCl_3$.

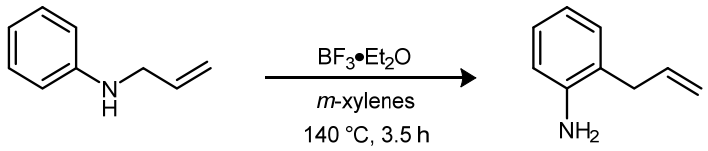

2-allylaniline. The following procedure was adapted from a previously reported method. In an N_2 filled glovebox, a Schlenk tube was charged with N-allylaniline (532 mg, 4 mmol, 1.0 equiv) and *m*-xylenes (10 mL). The Schlenk tube was sealed, removed from the glovebox and BF_3•Et_2O (490 uL, 4 mmol, 1.0 equiv) was added by syringe. The reaction mixture was heated at 140 °C. After 3 h, the mixture was cooled to room temperature and diluted with 10 mL of aqueous NaOH. The solution was extracted with 3 × 10 mL of EtOAc. The combined organic phases were washed with 10 mL of sat. NaCl (aq), dried over Na_2SO_4, and concentrated under reduced pressure. The product was isolated as a yellow oil. (370 mg, 70% yield). The spectral data match those previously reported.[3]

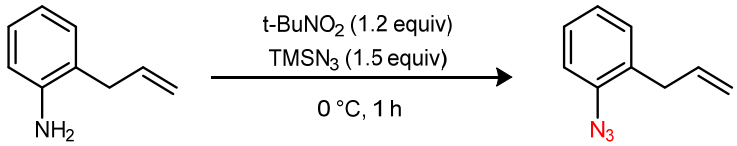

1-allyl-2-azidobenzene. A solution of 2-allylaniline (0.370 g, 2.7 mmol, 1.0 equiv) in CH_3CN (5 mL) was cooled to 0 °C. *t*-$BuNO_2$ (0.5 mL, 1.2 equiv) and $TMSN_3$ (0.45 mL, 1.5 equiv) were added sequentially. The reaction mixture was vigorously stirred at room temperature under air for 1 h. The mixture was concentrated to dryness under reduced pressure. The crude product was directly loaded onto a SiO_2 column for purification (50:50 DCM:hexanes). The product was isolated as a yellow oil (0.380 g, 86% yield). The spectral data match those previously reported.[3]

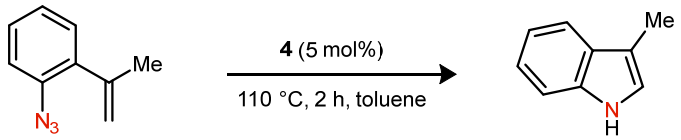

12 (70% Yield)

Catalytic amination of 1-azido-2-(prop-1-en-2-yl)benzene with 4. In an N_2 filled glovebox, a J-Young NMR tube was charged with **4** (1.4 mg, 0.0013 mmol, 5 mol%), 1-azido-2-(prop-1-en-2-yl)benzene (4.0 mg, 0.026 mmol), 1,3,5-trimethoxybenzene (1.0 mg, 0.006 mmol) as an internal standard, and toluene-d_8 (700 µL). The reaction was heated at 110 °C for 2 h. The yield of indole was determined by ^{1}H NMR integration against the internal standard (70% yield). The spectral data match those previously reported.[4]

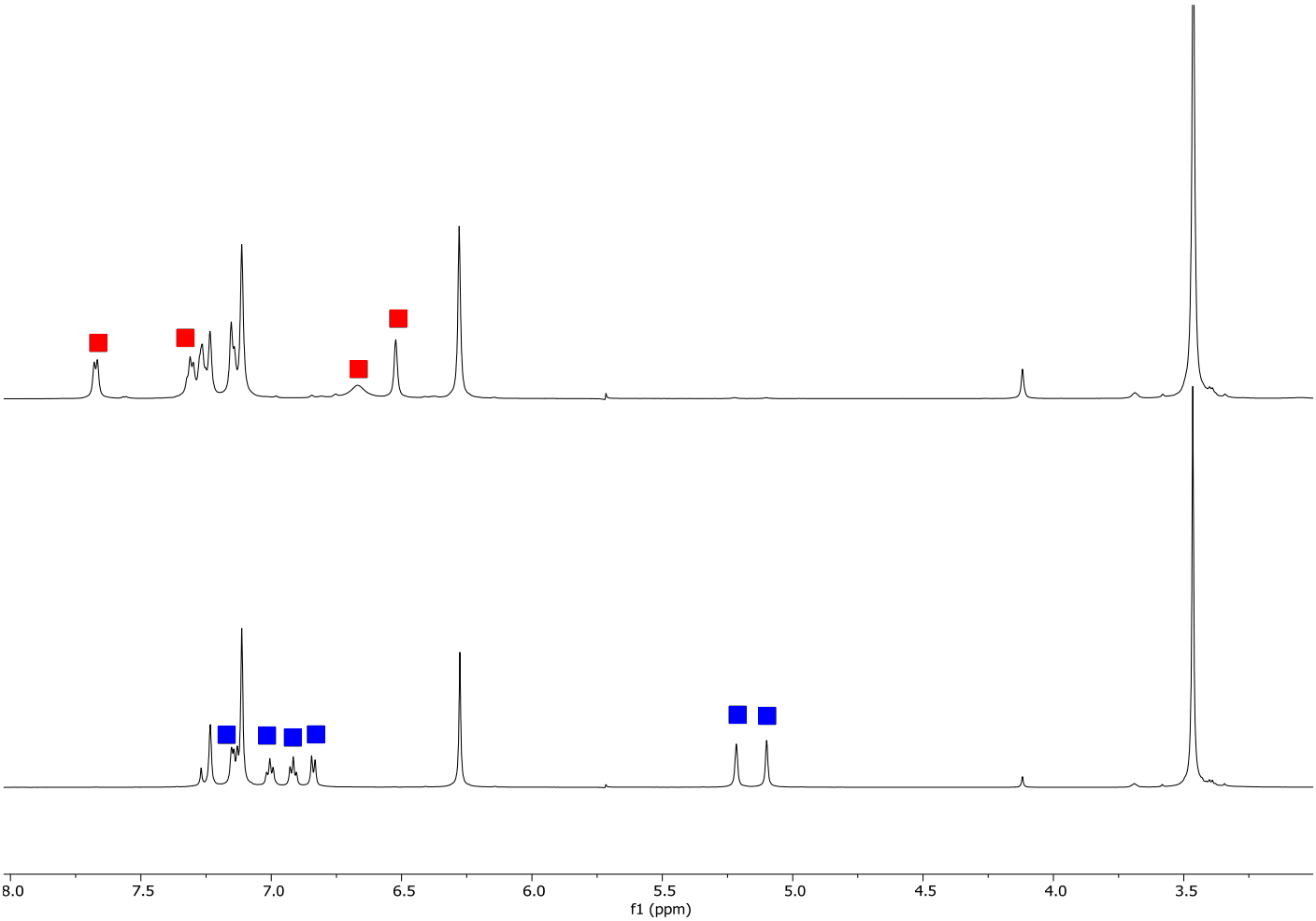

Figure S22. Bottom: ^{1}H NMR spectrum of 1-azido-2-(prop-1-en-2-yl)benzene. Top: ^{1}H NMR spectrum for the product mixture. Blue squares indicate starting material and red squares indicate **12**.

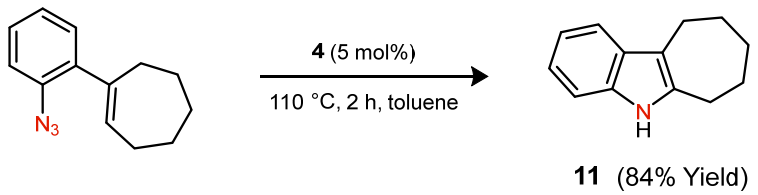

11 (84% Yield)

Catalytic amination of 1-(2-azidophenyl)cyclohept-1-ene with 4. In an N_2 filled glovebox, a J-Young NMR tube was charged with **4** (1.4 mg, 0.0013 mmol, 5 mol%), 1-(2-azidophenyl)cyclohept-1-ene (5.4 mg, 0.026 mmol), 1,3,5-trimethoxybenzene (1.0 mg, 0.006 mmol) as an internal standard, and toluene-d_8 (700 µL). The reaction was heated to 110 °C for 2 h. The yield of indole was determined by ^{1}H NMR integration against the internal standard (84% yield). The spectral data match those previously reported.[5]

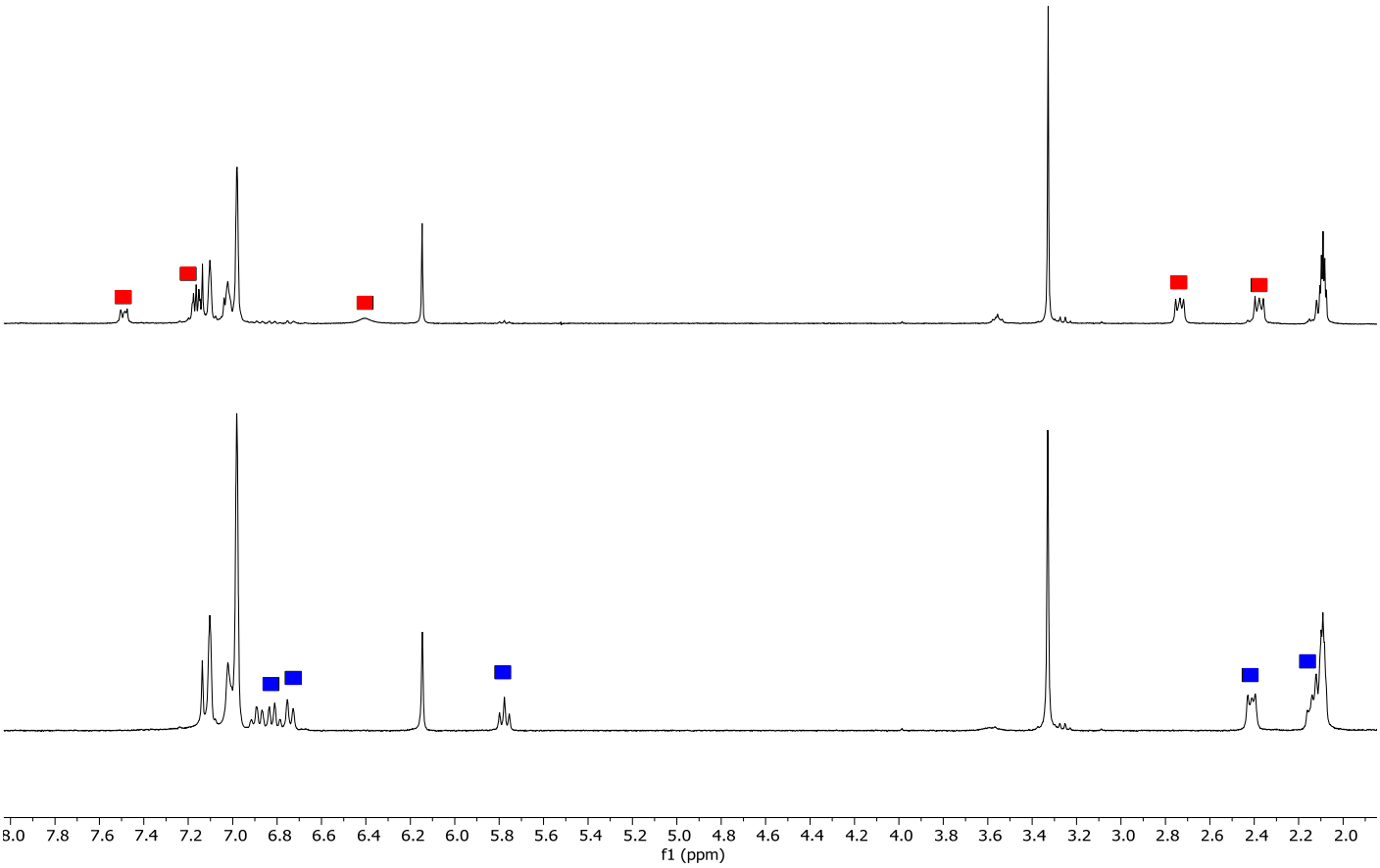

Figure S23. Bottom: ^{1}H NMR spectrum of 1-(2-azidophenyl)cyclohept-1-ene. Top: ^{1}H NMR spectrum of the product mixture. Blue squares indicate 1-(2-azidophenyl)cyclohept-1-ene and red squares indicate **11**.

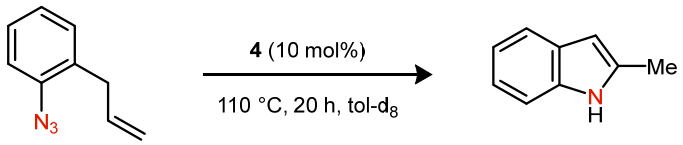

20 (61% Yield)

Catalytic amination of 1-allyl-2-azidobenzene with 4. In an N_2 filled glovebox, a J-Young NMR tube was charged with **4** (1.4 mg, 0.00126 mmol, 10 mol%), 1-allyl-2-azidobenzene (2.15 mg, 0.0135 mmol), 1,3,5-trimethoxybenzene (1.5 mg, 0.00892 mmol) as an internal standard, and toluene-d_8 (700 µL). The reaction was heated at 110 °C for 20 h. The yield of 2-methylindole was determined by ^{1}H NMR integration against the internal standard (61% yield). The spectral data match those previously reported.[6]

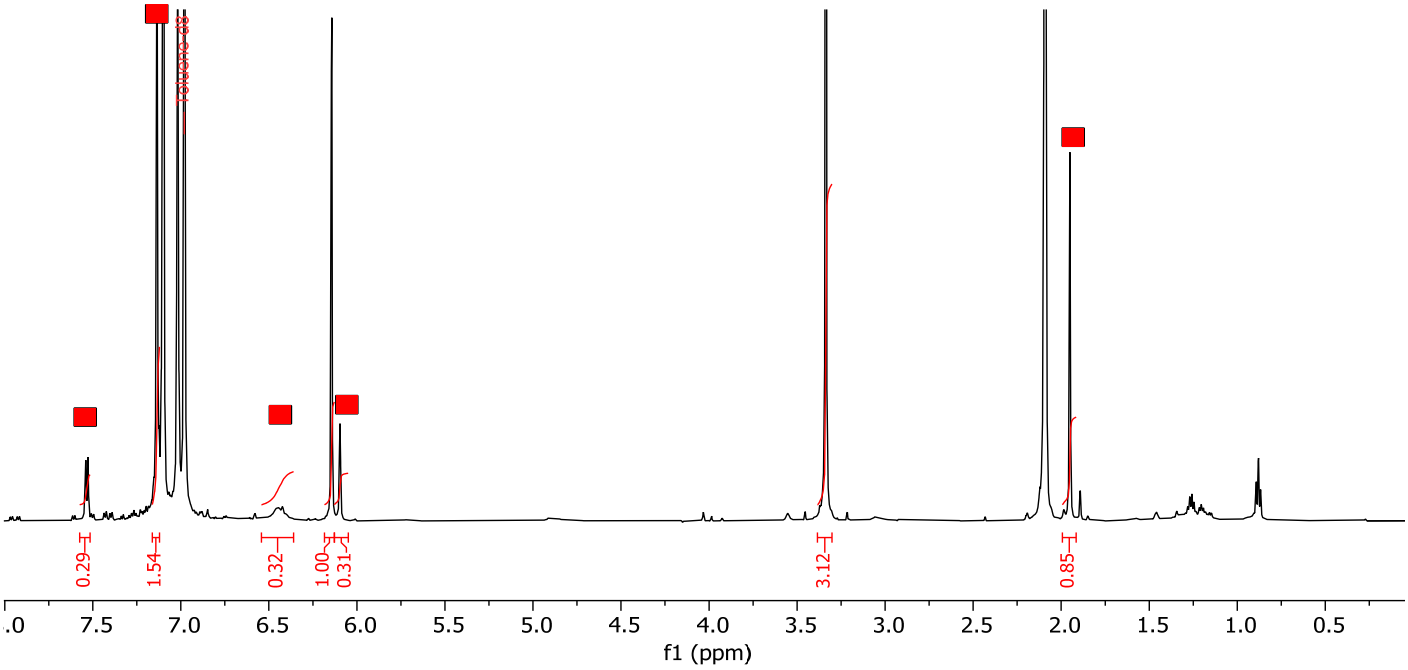

Figure S24. ^{1}H NMR spectrum of the product mixture. Red squares indicate **20**.

5. Mechanistic Experiments

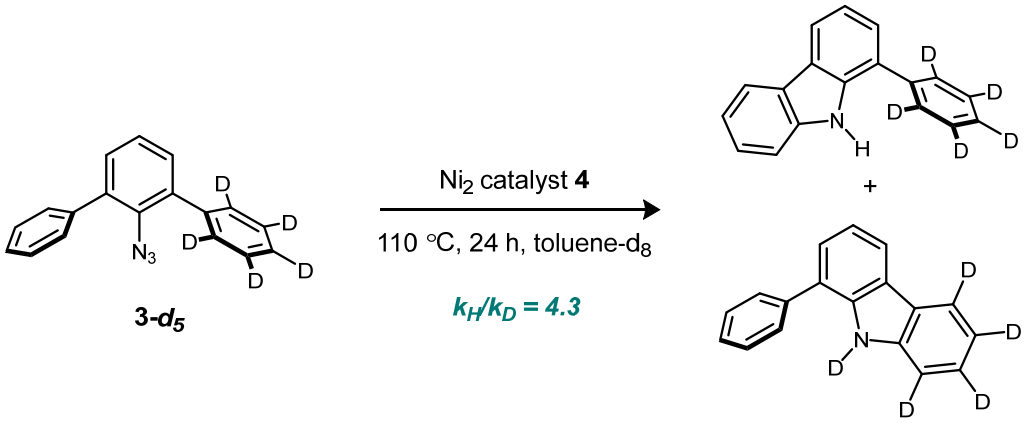

Catalytic amination of *m*-terphenylazide-d_5 with 4. In an N_2 filled glovebox, a J-Young NMR tube was charged with **4** (0.7 mg, 0.0007 mmol, 5 mol%), *m*-terphenylazide-d_5 (3.8 mg, 0.014 mmol, 1 equiv), and toluene-d_8 (700 µL). The reaction was heated at 110 °C for 24 h. The kinetic isotope effect was found to be 4.3 as determined by ^{1}H NMR integration. The spectral data match those previously reported.[7]

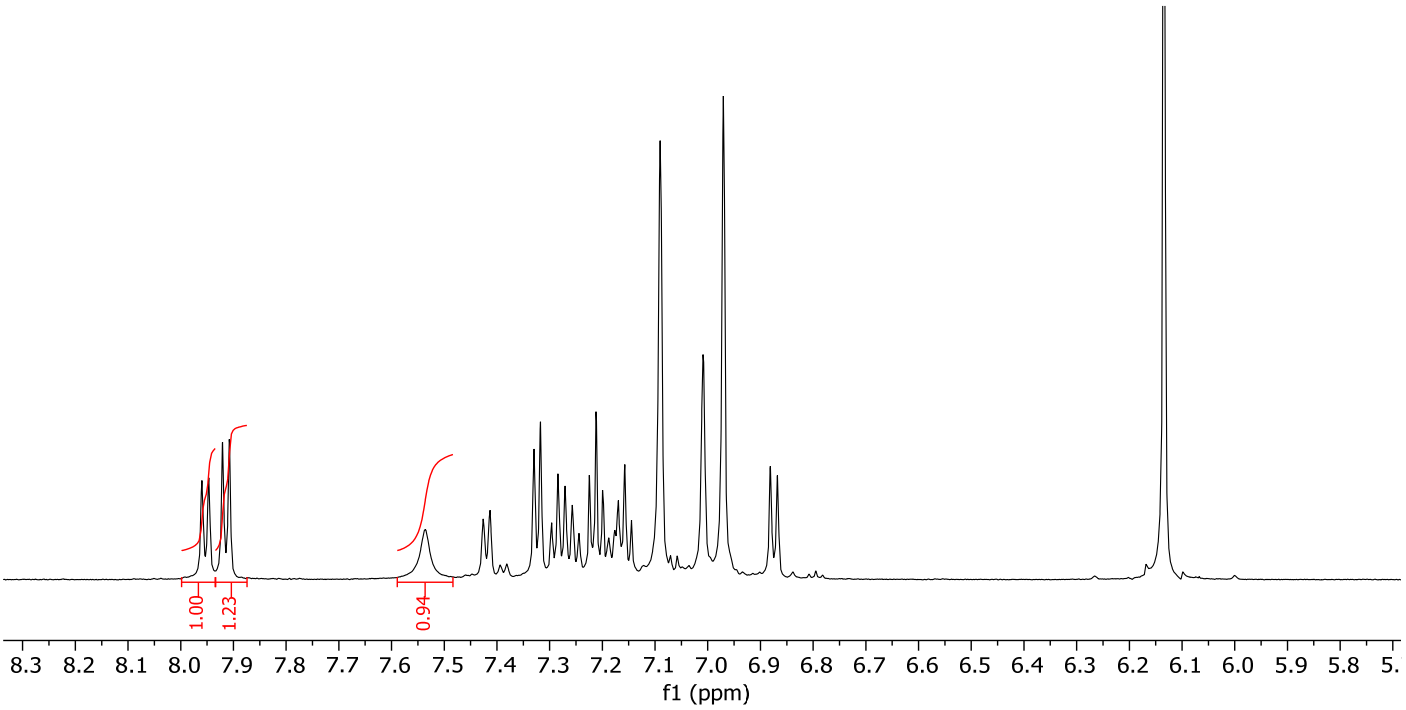

Figure S25. ^{1}H NMR spectrum of the amination of *m*-terphenylazide-d_5.

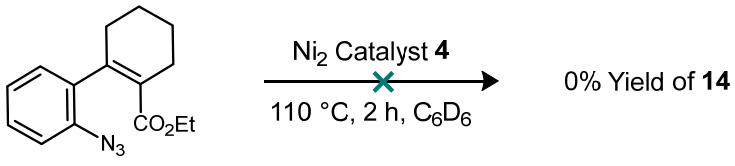

13

Catalytic amination of ethyl 2'-azido-3,4,5,6-tetrahydro-[1,1'-biphenyl]-2-carboxylate with 4. In an N_2 filled glovebox, a J-Young NMR tube was charged with **4** (1.4 mg, 0.0013 mmol, 10 mol%), **13** (3.4 mg, 0.013 mmol), 1,3,5-trimethoxybenzene (2.4 mg, 0.014 mmol) as an internal standard, and toluene-d_8 (825 µL).[8] The reaction was heated at 110 °C for 24 h. 15% conversion of azide **13** was observed, but **14** was not found in the reaction mixture.

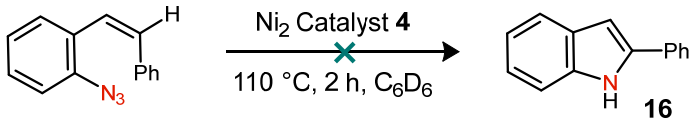

15-*Z* **16**

Catalytic amination of 15-*Z* with 4. In an N_2 filled glovebox, a J-Young NMR tube was charged with **4** (1.4 mg, 0.0013 mmol, 10 mol%), **15-*Z*** (2.8 mg, 0.013 mmol) 1,3,5-trimethoxybenzene (2.1 mg, 0.0013 mmol) as an internal standard, and toluene-d_8 (700 µL).[9] The reaction was heated at 110 °C for 2 h. The yield of indole was determined by ^{1}H NMR integration against the internal standard (0% yield).

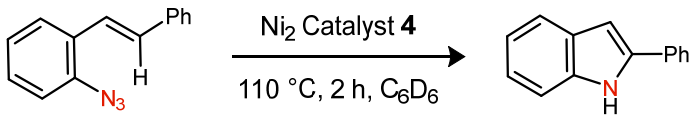

15-*E* **16**

Catalytic amination of 15-*E* with 4. In an N_2 filled glovebox, a J-Young NMR tube was charged with **4** (1.4 mg, 0.0013 mmol, 10 mol%), **15-*E*** (2.8 mg, 0.013 mmol), 1,3,5-trimethoxybenzene (2.1 mg, 0.0013 mmol) as an internal standard, and toluene-d_8 (700 µL). The reaction was heated at 110 °C for 2 h. The yield of indole was determined by ^{1}H NMR integration against the internal standard (>95% yield). The spectral data match those previously reported.[9]

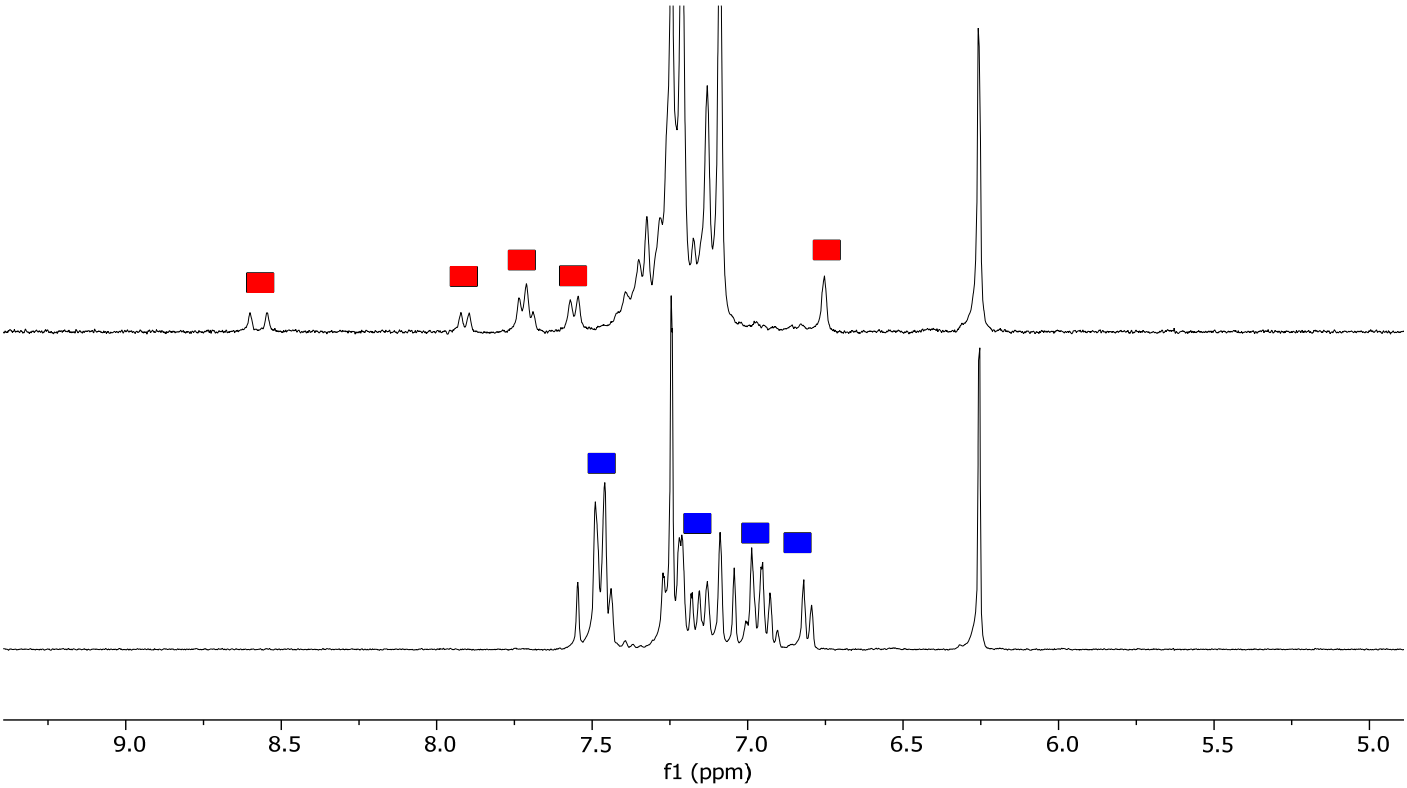

Figure S26. Bottom: ^{1}H NMR spectrum of **15-*E***. Top: ^{1}H NMR spectrum of product mixture. Blue squares indicate **15-E** and red squares indicate **16**.

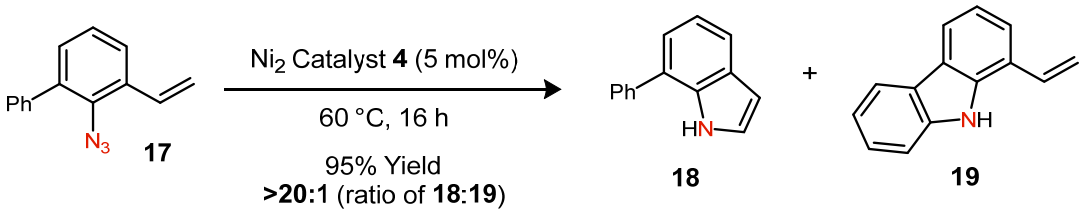

Catalytic amination of 17 with 4. In an N_2 filled glovebox, a J-Young NMR tube was charged with **4** (1.4 mg, 0.0013 mmol, 5 mol%), **17** (5.6 mg, 0.013 mmol), 1,3,5-trimethoxybenzene (2.1 mg, 0.0013 mmol) as an internal standard, and toluene-d_8 (700 µL). The reaction was heated at 110 °C for 2 h. The yield of indole was determined by ^{1}H NMR integration against the internal standard (95% yield). The spectral data match those previously reported.[10]

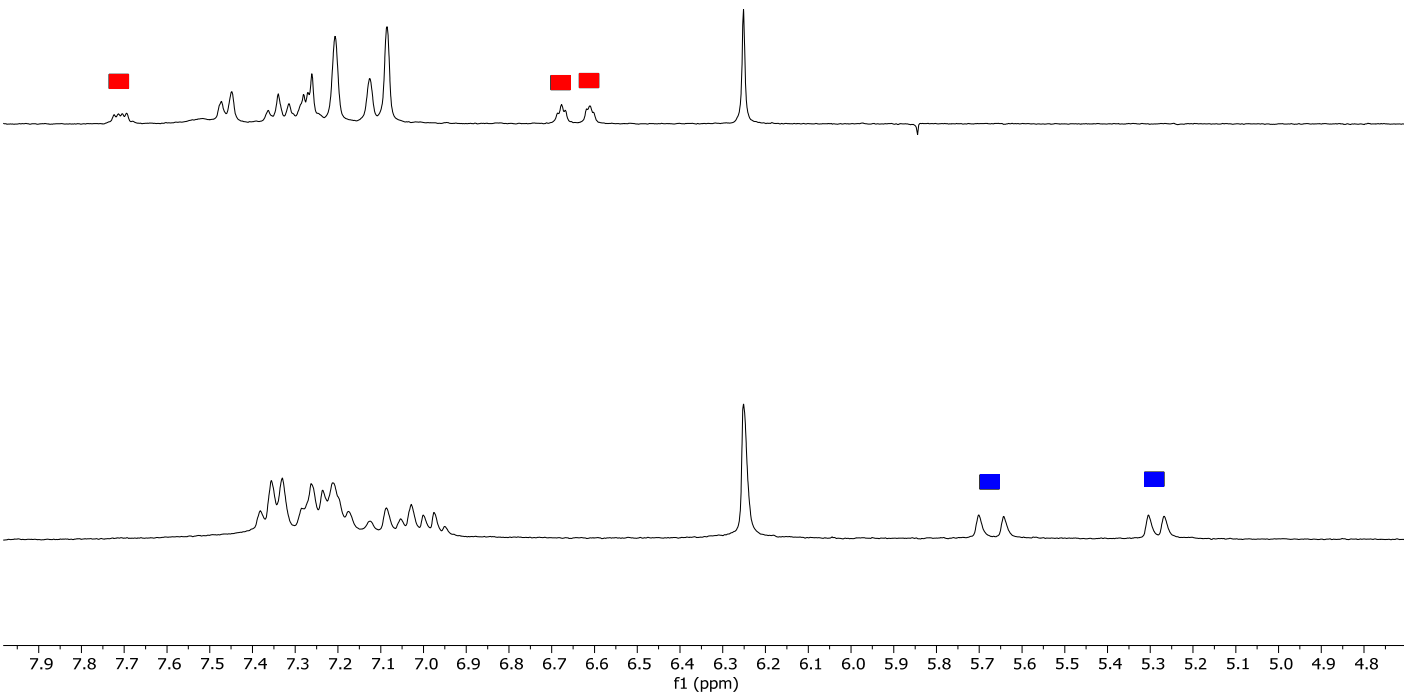

Figure S27. Bottom: ^{1}H NMR spectrum of **17**. Top: ^{1}H NMR spectrum of the product mixture. Blue squares indicate **17** and red squares indicate **18**.

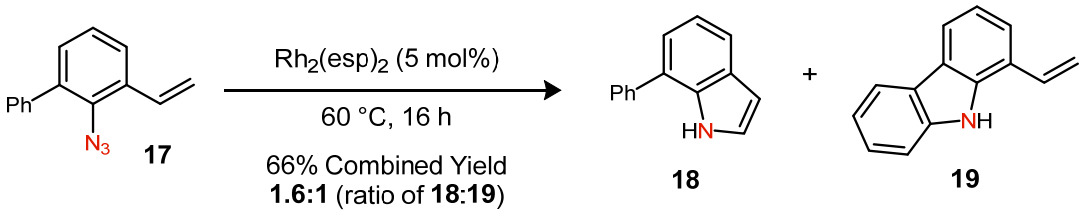

Catalytic amination of 17 with $Rh_2(esp)_2$ (5% loading). In an N_2 filled glovebox, a conical microwave vial was charged with $Rh_2(esp)_2$ (4.6 mg, 0.0061 mmol, 5 mol%), **17** (27 mg, 0.12 mmol), 1,3,5-trimethoxybenzene (2.1 mg, 0.0013 mmol) as an internal standard, and toluene (0.24 mL). The reaction was heated at 60 °C for 16 h after which the solvent was removed under reduced pressure. The yield of indole was determined by ^{1}H NMR integration against the internal standard (66% combined yield of **18** and **19** in a 1.6:1 ratio respectively). The spectral data match those previously reported.[11]

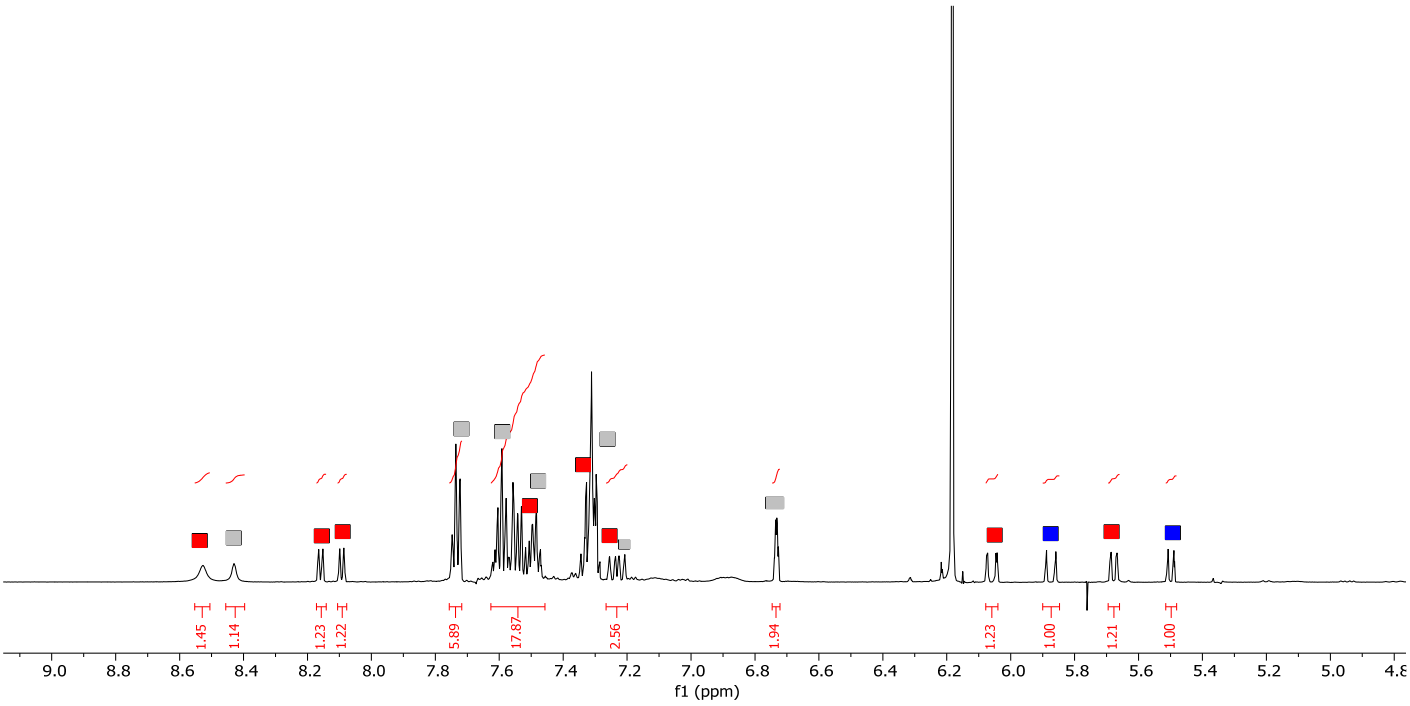

Figure S28. ^{1}H NMR spectrum of the product mixture. Blue squares indicate peaks corresponding to **17**, grey squares indicate peaks corresponding to **18** and red square indicates peaks corresponding to **19**.

6. X-Ray Diffraction Data

X-Ray Crystallography Data Processing. All data sets were processed using HKL3000 and data were corrected for absorption and scaled using Scalepack.[12] The space groups were assigned using XPREP from the Shelxtl suite of programs,[13] and structures were solved by direct methods using SHELXS and refined against F^2 on all data by full-matrix least-squares. The graphical user interface ShelXle[14] was used for refinement with the SHELXL program.[15] H-atoms attached to carbons were positioned geometrically and constrained to ride on their parent atoms, with carbon–hydrogen bond distances of 0.95 Å for and aromatic C–H, 1.00, 0.99 and 0.98 Å for aliphatic C–H, CH_2 and CH_3 moieties, respectively. Methyl H-atoms were allowed to rotate but not tip to best fit the experimental electron density. Positions of amine H-atoms were refined. U_{iso}(H) values were set to a multiple of U_{eq}(C/N) with 1.5 for CH_3, and 1.2 for C–H, CH_2 and N–H units, respectively. Complete crystallographic data, in CIF format, have been deposited with the Cambridge Crystallographic Data Centre. CCDC 1907259, 1907257, 1907253 contains the supplementary crystallographic data for this paper. These data can be obtained free of charge from The Cambridge Crystallographic Data Centre via www.ccdc.cam.ac.uk/data_request/cif.

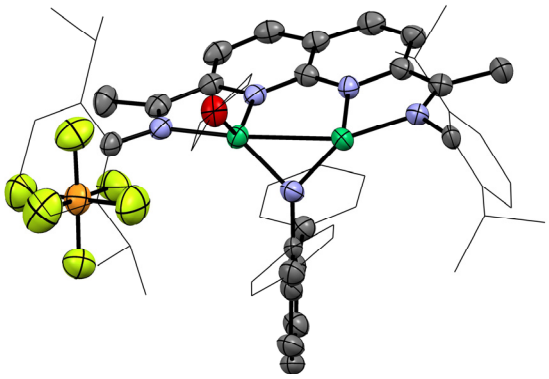

Compound 4

Crystal data	
Chemical formula	$C_{68}H_{85}F_6N_5Ni_2O_{3.50}P$
M_r	1290.79
Crystal system, space group	Monoclinic, $P2_1/n$
Temperature (K)	100
a, b, c (Å)	20.815 (4), 11.898 (2), 25.361 (5)
β (°)	94.16 (3)
V (Å^3)	6264 (2)
Z	4
Radiation type	Cu $K\alpha$
μ (mm^{-1})	1.56
Crystal size (mm)	0.60 × 0.20 × 0.02

Data collection	
Diffractometer	Rigaku Rapid II curved image plate diffractometer
Absorption correction	Multi-scan *SCALEPACK* (Otwinowski & Minor, 1997)
T_{min}, T_{max}	0.831, 0.969
No. of measured, independent and observed [$I > 2\sigma(I)$] reflections	64590, 11706, 7706
R_{int}	0.072
$(\sin \theta/\lambda)_{max}$ (Å^{-1})	0.617
Refinement	
$R[F^2 > 2\sigma(F^2)]$, $wR(F^2)$, S	0.078, 0.219, 1.07
No. of reflections	11706
No. of parameters	804
No. of restraints	10
H-atom treatment	H-atom parameters constrained
	$w = 1/[\sigma^2(F_o^2) + (0.0767P)^2 + 20.3456P]$ where $P = (F_o^2 + 2F_c^2)/3$
$\Delta\rho_{max}$, $\Delta\rho_{min}$ (e Å^{-3})	1.03, -0.63

*The three THF molecules were refined as disordered. One around an inversion center in a 1:1 ratio (that of O3). The other two (of O2 and O4) as disordered over two moieties in general positions. All disordered THF moieties were restrained to have similar geometries as that of a not disordered Ni-coordinated THF molecule. U^{ij} components of ADPs for disordered atoms closer to each other than 2.0 Angstrom were restrained to be similar. Subject to these conditions the occupancy ratio refined to 0.536(11) to 0.464(11) for the THF of oxygen O2, and to 0.724(9) to 0.276(9) for the THF of oxygen O4. Several reflections were located behind the beam stop, and were therefore omitted.

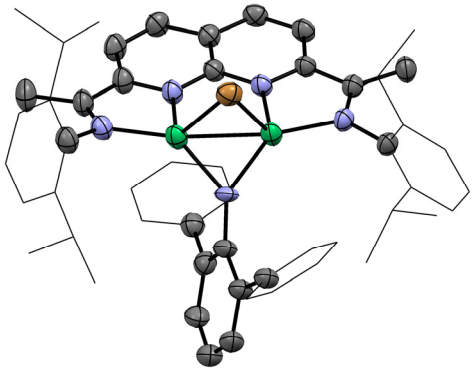

Compound 6

Crystal data	
Chemical formula	$0.8843(C_{56}H_{62}BrN_4Ni_2)\cdot 0.1157(C_{36}H_{57}Br_2N_5Ni_2)\cdot 2(C_4H_8O)$
M_r	1098.38
Crystal system, space group	Monoclinic, $P2_1/n$
Temperature (K)	100
a, b, c (Å)	18.650 (4), 27.977 (6), 21.577 (4)
β (°)	104.92 (3)
V (Å^3)	10879 (4)
Z	8
Radiation type	Cu $K\alpha$
μ (mm^{-1})	2.18
Crystal size (mm)	0.50 × 0.20 × 0.10
Data collection	
Diffractometer	Rigaku Rapid II curved image plate diffractometer
Absorption correction	Multi-scan *SCALEPACK* (Otwinowski & Minor, 1997)
T_{min}, T_{max}	0.831, 0.969
No. of measured, independent and observed [$I > 2\sigma(I)$] reflections	101438, 19994, 15997
R_{int}	0.089
$(\sin\theta/\lambda)_{max}$ (Å^{-1})	0.618
Refinement	
$R[F^2 > 2\sigma(F^2)]$, $wR(F^2)$, S	0.069, 0.186, 1.03
No. of reflections	19994
No. of parameters	1476
No. of restraints	772
H-atom treatment	H-atom parameters constrained

	$w = 1/[\sigma^2(F_o^2) + 33.1064P]$ where $P = (F_o^2 + 2F_c^2)/3$
$\Delta\rho_{max}$, $\Delta\rho_{min}$ (e Å^{-3})	1.29, -0.82

*The structure contains a number of disordered THF molecules. These molecules were refined with variable occupancies and restrained using SIMU and SAME commands.

The structure also contains a disorded Br atom due to cocrystallization with a dibromide species. The position of this atom was constrained with a SADI command to match the NiBr distances present for the nondisordered Br atom, and its occupancy was freely refined to a value of 0.1055(18).

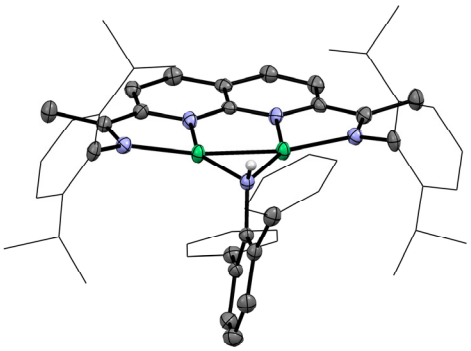

Compound 8

Crystal data	
Chemical formula	$C_{54}H_{58}N_5Ni_2 \cdot 3(C_6H_6)$
M_r	1128.79
Crystal system, space group	Triclinic, $P\bar{1}$
Temperature (K)	100
a, b, c (Å)	10.0447 (4), 16.2257 (6), 19.2830 (7)
α, β, γ (°)	86.007 (2), 75.110 (3), 78.833 (3)
V (Å^3)	2979.1 (2)
Z	2
Radiation type	Cu $K\alpha$
μ (mm^{-1})	1.14
Crystal size (mm)	0.40 × 0.05 × 0.01
Data collection	
Diffractometer	Rigaku Rapid II curved image plate diffractometer
Absorption correction	Multi-scan *SCALEPACK* (Otwinowski & Minor, 1997)
T_{min}, T_{max}	0.750, 0.989
No. of measured, independent and observed [$I > 2\sigma(I)$] reflections	9411, 9411, 7497
R_{int}	0.076
$(\sin \theta/\lambda)_{max}$ (Å^{-1})	0.580
Refinement	
$R[F^2 > 2\sigma(F^2)]$, $wR(F^2)$, S	0.055, 0.152, 1.06
No. of reflections	9411
No. of parameters	725
No. of restraints	1
H-atom treatment	H atoms treated by a mixture of independent and constrained

	refinement
$\Delta\rho_{max}$, $\Delta\rho_{min}$ (e Å^{-3})	0.61, -0.50

7. DFT Calculations and Optimized Structures

Computational Methods. Geometry optimizations were performed using the Gaussian09 software package.[16] All geometries were fully optimized at the BP86/6-311G(d,p) level of DFT. Stationary points were verified by frequency analysis. Isopropyl groups on the catalyst were truncated to methyl groups. A polarizable continuum model (PCM) was used to apply solvent corrections for S = 1/2 compounds.

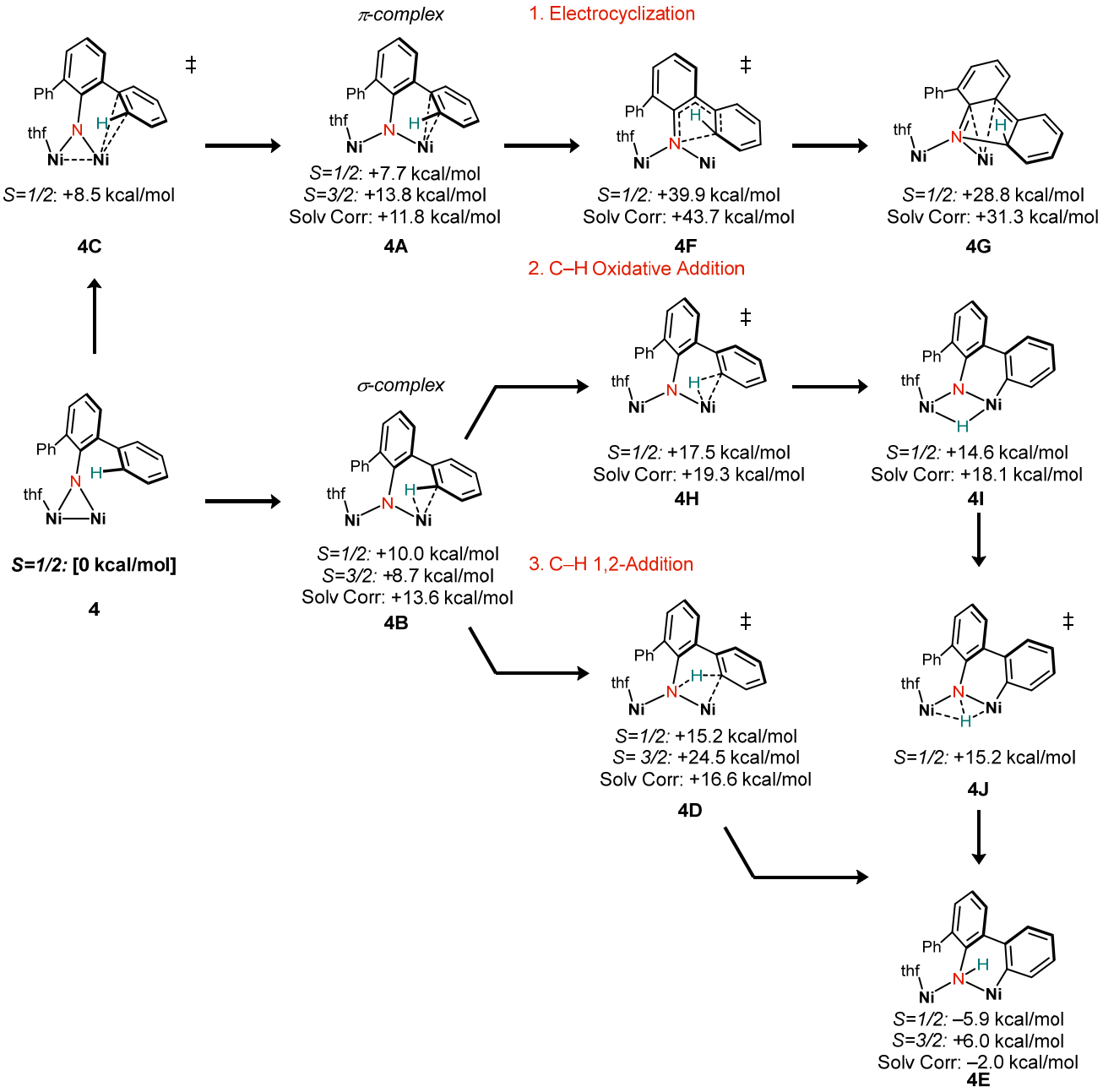

Figure S29. Reaction coordinate for electrocyclization, C–H oxidative addition and C–H 1,2-addition mechanisms of **4**. S=1/2 and S=3/2 spin states shown for C–H 1,2–Addition pathway (structures 4A-4E and 4J-4K). Energies are ΔG values at 383 K relative to that of **4** (BP86/6-31G(d,p) level of theory). Solvent corrections were applied to the S = 1/2 energies using the PCM(toluene) method.

Doublet:

Complex	NBO Ni 1	NBO Ni 2
4	9.19	9.05
4B	9.04	9.06
4D	9.04	9.16
4E	9.06	9.17

Figure S30. Natural Bond Orbital (NBO) analysis on Ni for each structure in the S=1/2 C–H 1,2-addition pathway. All complexes are best approximated as being Ni(I)/Ni(I).

Attempted Reductive Eliminations for C–H Oxidative Addition:

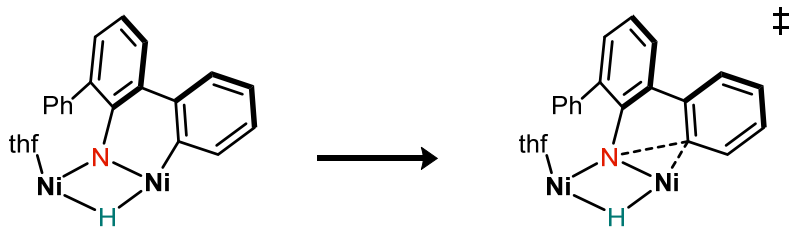

S=1/2: +14.6 kcal/mol **4I** *S=1/2:* +31.9 kcal/mol **4K**

Attemped Reductive Elimination for C–H 1,2-Addition:

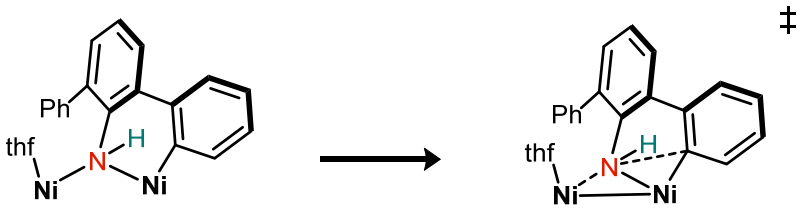

S=1/2: –5.9 kcal/mol **4E** *S=1/2:* +37.5 kcal/moll **4L**

Figure S31. Reductive elimination transition states were located but found to be too high in energy to be relevant to the reaction. Energies are ΔG values at 383 K relative to that of **4** (BP86/6-31G(d,p) level of theory).

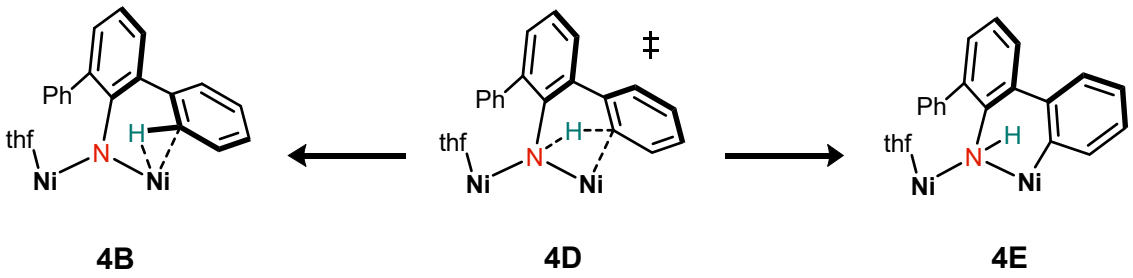

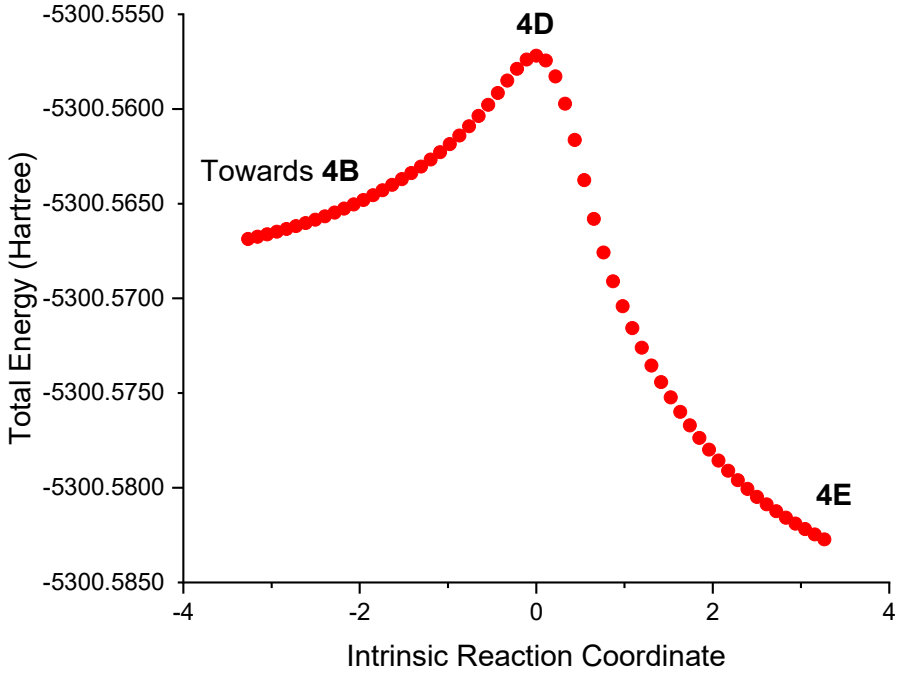

Figure S32. Intrinsic Reaction Coordinate (IRC) calculation for C–H 1,2-addition transition state **4D** with THF as ligand**.** Total energy of **4B** and **4E** are –5300.56918240 Hartrees and –5300.59440163 Hartrees respectively.

Complex 6

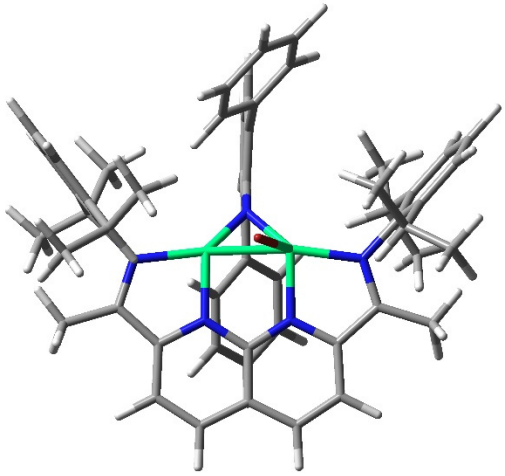

Charge: 0
Multiplicity: 2
Imaginary Frequencies: 0
Electronic Energy: –7640.314170 Hartrees
Gibbs Free Energy (353K): –7639.697760 Hartrees
Zero-Point Vibrational Energy: 1924830.3 J/mol

Charge: 0
Multiplicity: 4
Imaginary Frequencies: 0
Electronic Energy: –7640.297325 Hartrees
Gibbs Free Energy (353K): –7639.684274 Hartrees
Zero-Point Vibrational Energy: 1921737.5 J/mol

Complex 4

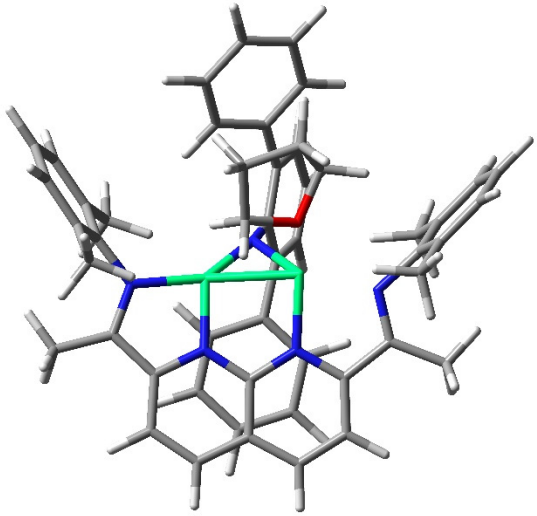

Charge: 1
Multiplicity: 2
Imaginary Frequencies: 0
Electronic Energy: –5300.58269527 Hartrees
Gibbs Free Energy (383K): –5299.869385 Hartrees
Zero-Point Vibrational Energy (H): 2230882.4 J/mol (D): 2222445.5 J/mol
Solvent Corrected Gibbs Free Energy (383K): –5299.900920 Hartrees

Charge: 1
Multiplicity: 4
Imaginary Frequencies: 0
Electronic Energy: –5300.56441855 Hartrees
Gibbs Free Energy (383K): –5299.854244 Hartrees
Zero-Point Vibrational Energy: 2228143.9 J/mol
Solvent Corrected Gibbs Free Energy (383K): –5299.882743 Hartrees

Complex 4C

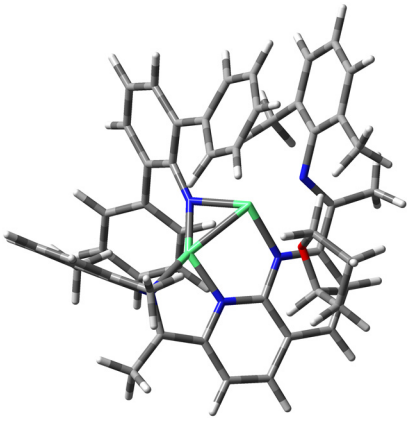

Charge: 1
Multiplicity: 2
Imaginary Frequencies: 1
Electronic Energy: –5300.561802 Hartrees
Gibbs Free Energy (383 K): –5299.855913 Hartrees
Zero-Point Vibrational Energy: 2227085.8 J/mol

Complex 4A

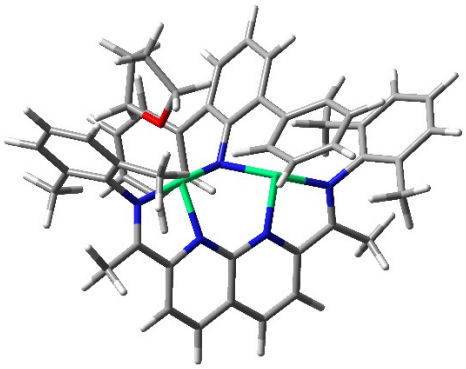

Charge: 1
Multiplicity: 2
Imaginary Frequencies: 0
Electronic Energy: –5300.57301636 Hartrees
Gibbs Free Energy (383 K): –5299.857033 Hartrees
Zero-Point Vibrational Energy (H): 2232449.1 J/mol (D): 2223974.0 J/mol
Solvent Corrected Gibbs Free Energy (383K): –5299.882143 Hartrees

Charge: 1
Multiplicity: 4
Imaginary Frequencies: 0
Electronic Energy: –5300.56208320 Hartrees
Gibbs Free Energy (383 K): –5299.847361 Hartrees
Zero-Point Vibrational Energy: 2231150.1 J/mol

Complex 4B

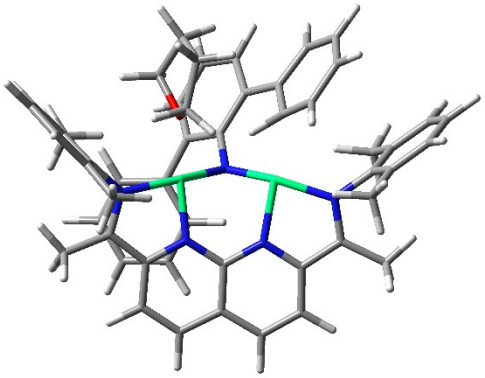

Charge: 1
Multiplicity: 2
Imaginary Frequencies: 0
Electronic Energy: –5300.56918240 Hartrees
Gibbs Free Energy (383 K): –5299.853418 Hartrees
Zero-Point Vibrational Energy: 2230811.4 J/mol
Solvent Corrected Gibbs Free Energy (383K): –5299.879253 Hartrees

Charge: 1
Multiplicity: 4
Imaginary Frequencies: 0
Electronic Energy: –5300.56649216 Hartrees
Gibbs Free Energy (383 K): –5299.855457 Hartrees
Zero-Point Vibrational Energy: 2229727.1 J/mol

Complex 4D

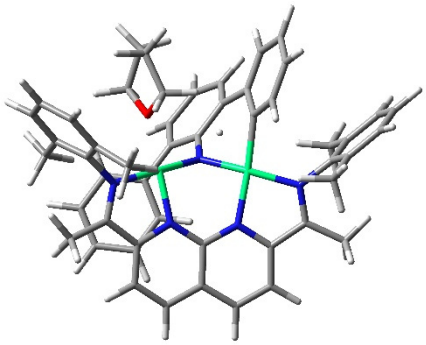

Charge: 1
Multiplicity: 2
Imaginary Frequencies: 1
Electronic Energy: –5300.55718006 Hartrees
Gibbs Free Energy (383 K): –5299.845158 Hartrees
Zero-Point Vibrational Energy (H): 2220379.6 J/mol (D): 2215647.6 J/mol
Solvent Corrected Gibbs Free Energy (383K): –5299.874423 Hartrees

Charge: 1
Multiplicity: 4
Imaginary Frequencies: 1
Electronic Energy: –5300.53754759 Hartrees
Gibbs Free Energy (383 K): –5299.830304 Hartrees
Zero-Point Vibrational Energy: 2215937.9 J/mol

Complex 4E

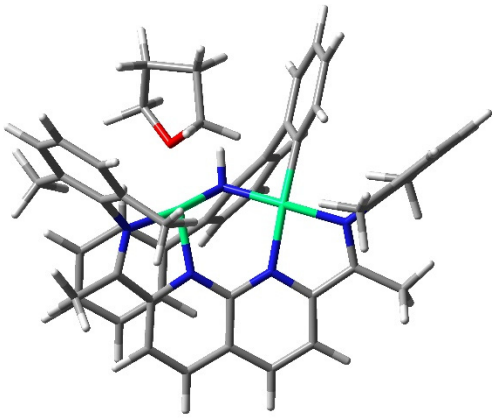

Charge: 1
Multiplicity: 2
Imaginary Frequencies: 0
Electronic Energy: –5300.59440163 Hartrees
Gibbs Free Energy (383 K): –5299.878758 Hartrees
Zero-Point Vibrational Energy: 2235482.2 J/mol
Solvent Corrected Gibbs Free Energy (383K): –5299.904157 Hartrees

Charge: 1
Multiplicity: 4
Imaginary Frequencies: 0
Electronic Energy: –5300.57471898 Hartrees
Gibbs Free Energy (383 K): –5299.859919 Hartrees
Zero-Point Vibrational Energy: 2232502.2 J/mol

Complex 4F

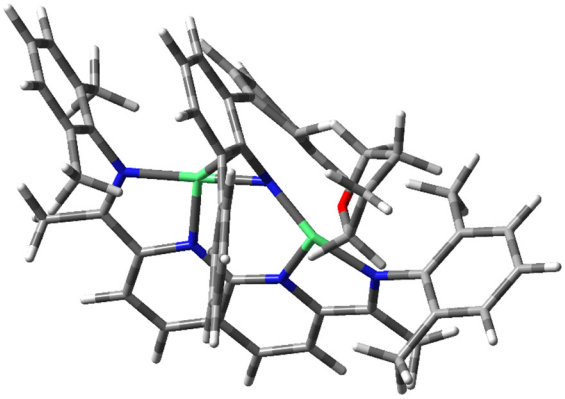

Charge: 1
Multiplicity: 2
Imaginary Frequencies: 1
Electronic Energy: -5300.524293 Hartrees
Gibbs Free Energy (383 K): –5299.805771 Hartrees
Zero-Point Vibrational Energy: 2229433.0 J/mol
Solvent Corrected Gibbs Free Energy (383K): – 5299.831341 Hartrees

Complex 4G

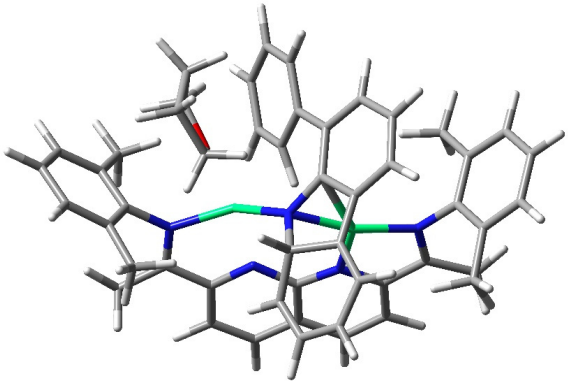

Charge: 1
Multiplicity: 2
Imaginary Frequencies: 0
Electronic Energy: –5300.53708234 Hartrees
Gibbs Free Energy (383 K): –5299.823556 Hartrees
Zero-Point Vibrational Energy: 2227739.6 J/mol
Solvent Corrected Gibbs Free Energy (383K): – 5299.850962 Hartrees

Complex 4H

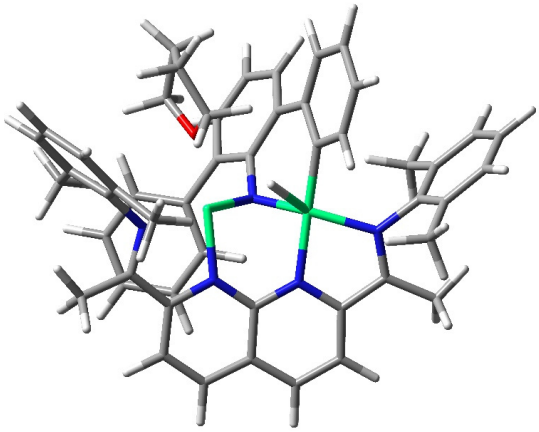

Charge: 1
Multiplicity: 2
Imaginary Frequencies: 1
Electronic Energy: –5300.55329722 Hartrees
Gibbs Free Energy (383 K): –5299.841473 Hartrees
Zero-Point Vibrational Energy: 2217681.3 J/mol
Solvent Corrected Gibbs Free Energy (383K): – 5299.870167 Hartrees

Complex 4I

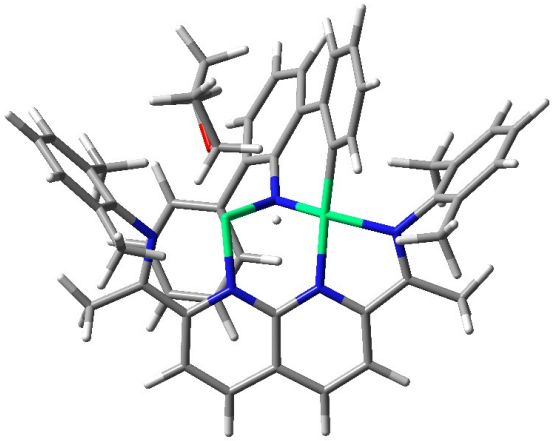

Charge: 1
Multiplicity: 2
Imaginary Frequencies: 0
Electronic Energy: –5300.55927500 Hartrees
Gibbs Free Energy (383 K): –5299.846078 Hartrees
Zero-Point Vibrational Energy: 2221073.4 J/mol
Solvent Corrected Gibbs Free Energy (383K): –5299.872011 Hartrees

Complex 4J

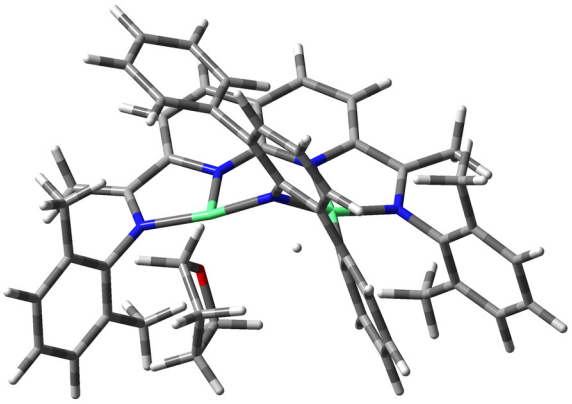

Charge: 1
Multiplicity: 2
Imaginary Frequencies: 1
Electronic Energy: –5300.557180 Hartrees
Gibbs Free Energy (383 K): –5299.845176 Hartrees
Zero-Point Vibrational Energy: 2220369.8J/mol
Solvent Corrected Gibbs Free Energy (383K): –5299.874486 Hartrees

Complex 4K

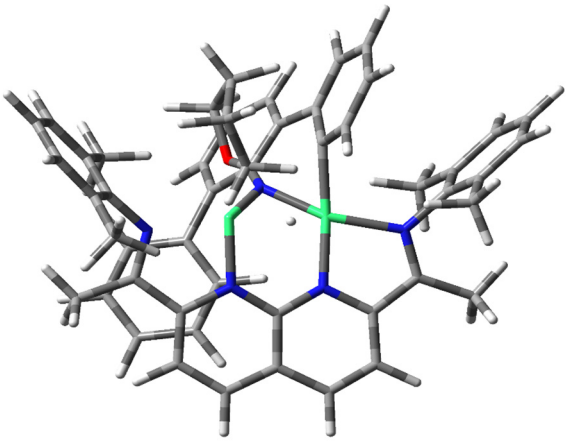

Charge: 1
Multiplicity: 2
Imaginary Frequencies: 1
Electronic Energy: –5300.530271 Hartrees
Gibbs Free Energy (383 K): –5299.818579 Hartrees
Zero-Point Vibrational Energy: 2219201.4 J/mol

Complex 4L

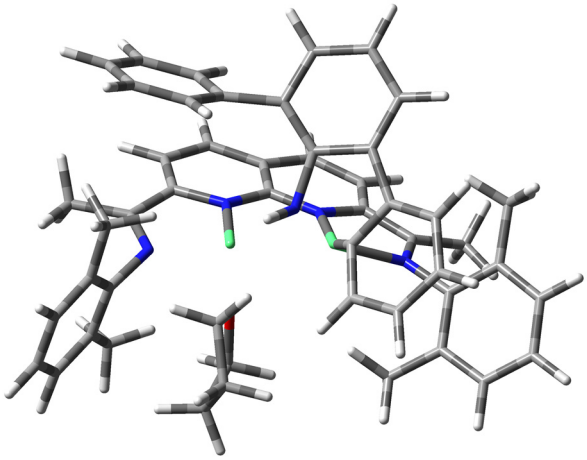

Charge: 1
Multiplicity: 2
Imaginary Frequencies: 1
Electronic Energy: –5300.523371 Hartrees
Gibbs Free Energy (383 K): – 5299.809567 Hartrees
Zero-Point Vibrational Energy: 2225778.3 J/mol

Charge: 1
Multiplicity: 4
Imaginary Frequencies: 1
Electronic Energy: –5300.523880 Hartrees
Gibbs Free Energy (383 K): –5299.809648 Hartrees
Zero-Point Vibrational Energy: 2226681.5 J/mol

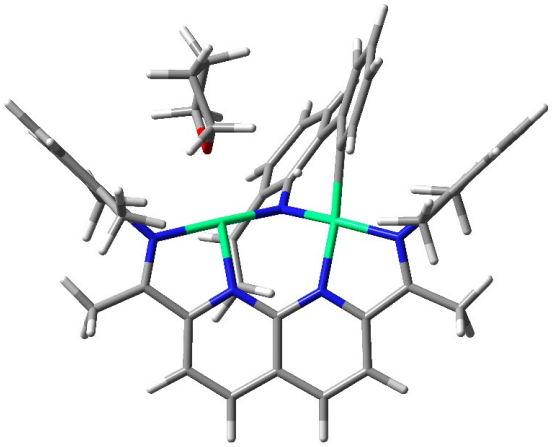

Charge: 1
Multiplicity: 2
Imaginary Frequencies: 1
Electronic Energy: –5146.89724466 Hartrees
Gibbs Free Energy (383.0 K): –5146.226867 Hartrees
Zero-Point Vibrational Energy: 2098137.0 J/mol

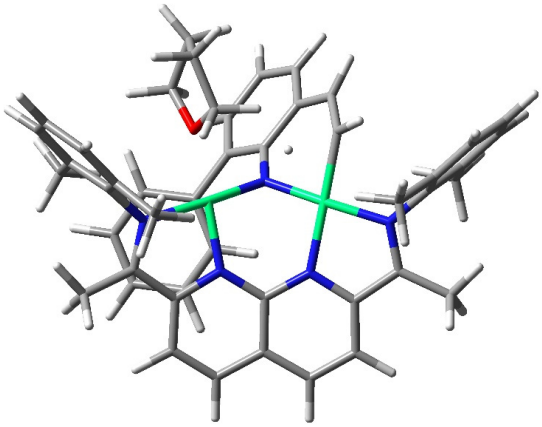

Charge: 1
Multiplicity: 2
Imaginary Frequencies: 1
Electronic Energy: –5146.91309061 Hartrees
Gibbs Free Energy (383.0 K): –5146.240588 Hartrees
Zero-Point Vibrational Energy: 2101424.1 J/mol

Complex 8

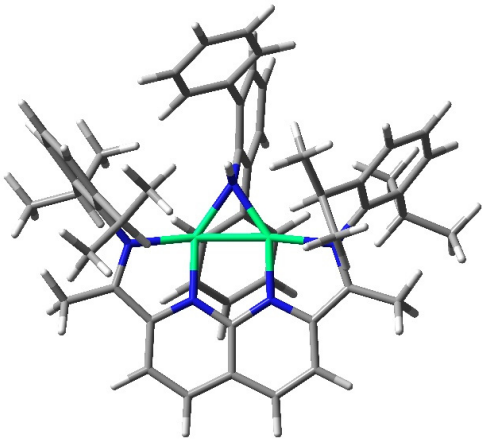

Charge: 0
Multiplicity: 2
Imaginary Frequencies: 0
Electronic Energy: –5383.40650269 Hartrees
Gibbs Free Energy (353 K): –5382.567691 Hartrees
Zero-Point Vibrational Energy: 2533082.6 J/mol

8. References

1. Youn, S. W.; Ko, T. Y.; Jang, M. J.; Jang, S. S. *Adv. Synth. Catal.* **2015**, *357*, 227–234.
2. Kong, C.; Jana, N.; Jones, C.; Driver, T. G. *J. Am. Chem. Soc.* **2016**, *138*, 13271–13280.
3. Brucelle, F.; Renaud, P. *Org. Lett*. **2012**, 14, 12, 3048–3051
4. He, K.-H.; Tan, F.-F.; Zhou, C.-Z.; Zhou, G.-J.; Yang, X.-L.; Li, Y.. *Angew. Chem., Int. Ed.* **2017**, *56*, 3080–3084.
5. Gore, S.; Baskaran, S.; König, B. *Org. Lett.* **2012**, *14* , 4568–4571.
6. Buil, M. L.; Esteruelas, M. A.; Gay, M. P.; Gomez-Gallego, M.; Nicasio, A. I.; Onate, E.; Santiago, A.; Sierra, M. A. *Organometallics* **2018**, 37, 4, 603–617
7. Powers, I. G.; Kiattisewee, C.; Mullane, K. C.; Schelter, E. J.; Uyeda, C. *Chem. Eur. J. **2017**, 23, 7694–7697.*
8. Kong, C.; Driver, T. G. *Org. Lett.* **2015**, *17*, 802–805.
9. Shen, M.; Leslie, B. E.; Driver, T. G. *Angew. Chem., Int. Ed.* **2008**, *47*, 5056–5059
10. Robbins, D. W.; Boebel, T. A.; Hartwig, J. F. *J. Am. Chem. Soc.* **2010**, *132*, 4068–4069.
11. Tsvelikhovsky, D.; Buchwald, S. L. *J. Am. Chem. Soc.* **2010**, *132*, 14048–14051.
12. Otwinowski, Z.; Minor, W. in: Methods Enzymol., 1997, pp. 307–326.
13. (a) SHELXTL (Version 6.14) (2000-2003) Bruker Advanced X-ray Solutions, Bruker AXS Inc., Madison, Wisconsin: USA. (b) Sheldrick, G. M. *Acta Cryst.* **2008**, A64, 112-122.
14. Hübschle, C. B.; Sheldrick, G. M.; Dittrich, B. *J. Appl. Crystallogr.* **2011**, *44,* 1281-1284.
15. Sheldrick, G. M. *Acta Crystallogr., Sect. C* **2015**, *71* 3-8.
16. Gaussian 09, Revision A.02, M. J. Frisch, G. W. Trucks, H. B. Schlegel, G. E. Scuseria, M. A. Robb, J. R. Cheeseman, G. Scalmani, V. Barone, G. A. Petersson, H. Nakatsuji, X. Li, M. Caricato, A. Marenich, J. Bloino, B. G. Janesko, R. Gomperts, B. Mennucci, H. P. Hratchian, J. V. Ortiz, A. F. Izmaylov, J. L. Sonnenberg, D. Williams-Young, F. Ding, F. Lipparini, F. Egidi, J. Goings, B. Peng, A. Petrone, T. Henderson, D. Ranasinghe, V. G. Zakrzewski, J. Gao, N. Rega, G. Zheng, W. Liang, M. Hada, M. Ehara, K. Toyota, R. Fukuda, J. Hasegawa, M. Ishida, T. Nakajima, Y. Honda, O. Kitao, H. Nakai, T. Vreven, K. Throssell, J. A. Montgomery, Jr., J. E. Peralta, F. Ogliaro, M. Bearpark, J. J. Heyd, E. Brothers, K. N. Kudin, V. N. Staroverov, T. Keith, R. Kobayashi, J. Normand, K. Raghavachari, A. Rendell, J. C. Burant, S. S. Iyengar, J. Tomasi, M. Cossi, J. M. Millam, M. Klene, C. Adamo, R. Cammi, J. W. Ochterski, R. L. Martin, K. Morokuma, O. Farkas, J. B. Foresman, and D. J. Fox, Gaussian, Inc., Wallingford CT, 2016.